



**EXPERIMENTAL INVESTIGATION OF TURBOJET THRUST
AUGMENTATION USING AN EJECTOR**

THESIS

David A. Hoffman, Captain, USAF

AFIT/GAE/ENY/07-M13

**DEPARTMENT OF THE AIR FORCE
AIR UNIVERSITY**

AIR FORCE INSTITUTE OF TECHNOLOGY

Wright-Patterson Air Force Base, Ohio

APPROVED FOR PUBLIC RELEASE; DISTRIBUTION UNLIMITED

The views expressed in this thesis are those of the author and do not reflect the official policy or position of the United States Air Force, Department of Defense, or the U. S. Government.

AFIT/GAE/ENY/07-M13

EXPERIMENTAL INVESTIGATION OF TURBOJET THRUST AUGMENTATION
USING AN EJECTOR

THESIS

Presented to the Faculty

Department of Aeronautical and Astronautical Engineering

Graduate School of Engineering and Management

Air Force Institute of Technology

Air University

Air Education and Training Command

In Partial Fulfillment of the Requirements for the
Degree of Master of Science in Aeronautical Engineering

David A. Hoffman, BSME

Captain, USAF

March 2007

APPROVED FOR PUBLIC RELEASE; DISTRIBUTION UNLIMITED.

AFIT/GAE/ENY/07-M13

EXPERIMENTAL INVESTIGATION OF TURBOJET THRUST AUGMENTATION
USING AN EJECTOR

David A. Hoffman, BSME
Captain, USAF

Approved:

 /SIGNED/
Paul I. King (Chairman)

13 Mar 2007
date

 /SIGNED/
Raymond C. Maple (Member)

13 Mar 2007
date

 /SIGNED/
Milton E. Franke (Member)

13 Mar 2007
date

Abstract

In recent years a significant number of commercially available small turbines have become available. At the same time unmanned aerial vehicles and smart munitions have decreased in size while their endurance needs have increased. With these new platform requirements comes the need for a propulsion system with reliability, good endurance and low acoustic signature. There has been much research accomplished in the area of steady cold flow primary sources, but little experimental work has been done using a gas turbine as a steady flow hot source. This investigation concerns the performance of an ejector driven by a small gas turbine. Aircraft applicability was a deciding factor in test geometry. Varying both engine throttle and the ejector's downstream distance resulted in peak augmentation values of nearly 1.4.

To my loving and always supportive wife and daughter

Acknowledgments

I would first like to thank my advisor, Dr. Paul King for the opportunity to perform research where I got my hands dirty. Dr. King, I appreciate your time and support on this journey. Thank you to my committee members, Dr. Milton Franke and Lt Col. Raymond Maple for helping me refine my work.

I have to thank Dr. Fred Schauer for giving me unlimited access to your lab. I extend a special thanks to Curtis Rice for always being willing to lend a hand and a sanity check to something I was about to try.

Certainly, I would not be where I am today without the love and support of my family. Thank you to my wife for not only proofreading this document *ad nauseam* but also always being there when I needed it no matter what. To my wonderful daughter, I can't wait to spend more time with you, watch you grow, and teach you all that I have learned.

Table of Contents

	Page
ABSTRACT.....	IV
ACKNOWLEDGMENTS	VI
TABLE OF CONTENTS	VII
LIST OF FIGURES	IX
LIST OF SYMBOLS	X
I. INTRODUCTION.....	1
MOTIVATION	1
RESEARCH OBJECTIVES.....	2
SIGNIFICANCE OF RESEARCH.....	2
II. BACKGROUND AND THEORY	4
OVERVIEW.....	4
THE EJECTOR.....	4
IDEAL EJECTOR ANALYSIS	5
<i>Steady flow source</i>	<i>11</i>
<i>Unsteady flow source.....</i>	<i>12</i>
RELATED RESEARCH	12
<i>Non-engine driven.....</i>	<i>13</i>
<i>Engine driven.....</i>	<i>14</i>
<i>Analytic.....</i>	<i>16</i>
THE GAS TURBINE ENGINE.....	16
CHAPTER SUMMARY	19
III. MATERIALS AND METHODOLOGY	20
OVERVIEW.....	20
D-BAY FACILITY	20
AIR SUPPLY SYSTEM	21
ENGINE THRUST STAND	21
INSTRUMENTATION	23
<i>D-Bay Instrumentation.....</i>	<i>24</i>
<i>Engine Instrumentation.....</i>	<i>24</i>
ENGINE.....	24
<i>Operation and maintenance.....</i>	<i>26</i>
ENGINE CONTROL SYSTEM.....	27
ENGINE ELECTRICAL SYSTEM	28
ENGINE FUEL SYSTEM.....	29
TEST PROCEDURES	30
TEST SETUP	32
CHAPTER SUMMARY	32
IV. RESULTS AND DISCUSSION.....	33
OVERVIEW.....	33
MODELING THE TURBINE.....	34

	Page
CALCULATION OF SECONDARY FLOW CONDITIONS	37
DATA SERIES ONE	39
DATA SERIES TWO	43
DATA SERIES THREE	46
CHAPTER SUMMARY	53
V. CONCLUSIONS AND RECOMMENDATIONS.....	54
CONCLUSIONS	54
RECOMMENDATIONS	54
BIBLIOGRAPHY	57
VITA.....	59

List of Figures

	Page
FIGURE 1. BASIC EJECTOR GEOMETRY	5
FIGURE 2. ENGINE-EJECTOR NAMING SCHEMATIC	6
FIGURE 3. ENGINE-EJECTOR CONTROL VOLUME	7
FIGURE 4. JETCAT, GAS TURBINE SCHEMATIC	17
FIGURE 5. IDEAL BRAYTON CYCLE P-V AND T-S DIAGRAMS.....	18
FIGURE 6. D-BAY THRUST STAND DIAGRAM	23
FIGURE 7. JETCAT P200 TURBINE.....	25
FIGURE 8. JETCAT ENGINE CONTROL SOFTWARE GUI.....	27
FIGURE 9. JETCAT ELECTRICAL SYSTEM.....	29
FIGURE 10. JETCAT FUEL SYSTEM	30
FIGURE 11. VARIATION OF ϕ WITH DOWNSTREAM DISTANCE AND THROTTLE PERCENTAGE	34
FIGURE 12. INLET CONTROL VOLUME FOR ADDITIVE DRAG	36
FIGURE 13. SERIES ONE TEST SETUP	39
FIGURE 14. SERIES ONE, X=12" SIDE VIEW	40
FIGURE 15. SERIES ONE, X=12" TOP VIEW	40
FIGURE 16. SERIES ONE, ENGINE BASELINE	41
FIGURE 17. COMPARISON OF ϕ FOR ACTUAL AND IDEAL EJECTOR SYSTEM	42
FIGURE 18. EFFECT OF X DISTANCE ON ϕ FOR BOTH ACTUAL AND IDEAL EJECTOR SYSTEMS	43
FIGURE 19. SERIES TWO X=0" SIDE VIEW	44
FIGURE 20. EFFECT OF X DISTANCE ON ϕ FOR ENGINE, COLLECTOR AND EJECTOR SYSTEM.....	45
FIGURE 21. THRUST AUGMENTATION VARIATION WITH MFR RATIO WITH COLLECTOR TUBE	46
FIGURE 22. CHOPPER WHEEL, GEOMETRY AND DIMENSIONS	47
FIGURE 23. SERIES THREE X=6"	48
FIGURE 24. PIV FLOW VISUALIZATION OF A STEADY JET AND A PULSED JET [2], BY PERMISSION	49
FIGURE 25. VORTEX RING WITH EJECTOR PROFILE YIELDING PEAK AUGMENTATION [9]	50
FIGURE 26. SERIES THREE THRUST AND RPM VS TIME, X=6"	51
FIGURE 27. MECHANICAL LOSSES VS. THROTTLE PERCENTAGE	52
FIGURE 28. VARIATION OF ϕ AS A FUNCTION OF THROTTLE FOR SERIES THREE WITH THE CHOPPER NOT ROTATING	52

List of Symbols

Acronyms

AFRL – Air Force Research Lab
ECU – Engine Control Unit
EGT – Exhaust Gas Temperature
GUI – Graphical User Interface
MFR – Mass Flow Rate
PDE – Pulse Detonation Engine
RPM – Revolutions Per Minute
TSFC – Thrust Specific Fuel Consumption
UAV – Unmanned Aerial Vehicle

Symbols

A – Area
D – Diameter
 Dh° – Substantial derivative of specific stagnation enthalpy
 Ds – Substantial derivative of specific entropy
Dt – Differential time
 \bar{f} – Shear forces from turbulent and viscous stresses
L – Length
 P, p – Pressure
T – Temperature
t – Time
U – Local fluid velocity
 \bar{u} – Local fluid velocity
V – Velocity
X – Ejector downstream distance, primary exit plane to secondary inlet plane
 α – Area ratio, cross-sectional area of primary over secondary cross-sectional area
 ϕ – Thrust augmentation, total system thrust over primary thrust
 ρ – Density

Subscripts

a – Ambient Conditions
ej – Ejector
p – Primary source
s – Secondary source
T – Primary stagnation condition
TOT – Total system

I. Introduction

Motivation

In response to the demand in the remote control model aviation segment there are now a significant number of commercially available small turbines on the market. At the same time the miniaturization of electronics has allowed for truly fantastic capabilities in both Unmanned Aerial Vehicles (UAV) and smart long loiter munitions. With these new platforms comes the need for a propulsion system with reliability, good endurance and low acoustic signature.

Ejectors, which have been studied for over sixty years, can offer reduced fuel consumption and noise levels as well as ease of operation. With ejectors, it can be shown that the type of primary source, either steady or unsteady, has a significant effect on the amount of augmentation gained. Recent research has shown that an unsteady primary source can result in thrust augmentation (ϕ) greater than two times the source [1], while steady augmentation will result in about 1.4 times the primary source [2,3].

Over the years, research on steady flow ejectors has focused mainly on cold steady flow primary jets. There has been little research concerning ejectors employed with gas turbines, a hot source, and still less dealing with small turbines. This is due in part to the difficulty and cost of running a large turbojet engine and the lack of a small-scale reliable turbine to use to power the ejector. Papers that focus on steady flow ejectors note that the work would be directly scalable to hot flow sources. Conversely,

there has been significant research on unsteady flow primary jets using the actual engines due to the smaller nature of the pulsejet and Pulsed Detonation Engines (PDE).

Research Objectives

The objective of this research was to both quantify experimentally the amount of augmentation an ejector will produce when driven with a small turbojet as the primary source and to explore novel ways to improve this augmentation.

Flight applicability was considered when choosing the basic test geometry. Although the turbine could have been setup inside the ejector, which would have been much more compact, this would not have allowed it to be jettisoned in flight. With the ejector located downstream, it could be jettisoned after takeoff. The flight regime of most small UAVs and loiter munitions either is or is planned to be low speed (< 0.3 Mach). Ejectors create peak augmentation at very low Mach numbers [4]. This allows ejectors to provide the increase in thrust and decrease in acoustic signature much needed by the small aircraft typifying today's UAVs and smart munitions.

Significance of Research

Air Force Research Labs Propulsion Directorate (AFRL/PR), develops propulsion and related technologies for the Air Force including: turbine and rocket engines, advanced propulsion systems, fuels, propellants, lubricants, and aircraft power. Dr. Fred Schauer of AFRL/PR, as thesis sponsor, is specifically interested in both reducing Thrust Specific Fuel Consumption (TSFC) and unsteady source thrust augmentation. Thrust augmentation using ejectors driven by an unsteady source is a very popular area of

research, as of late, due to the current interest in PDEs. Regarding small turbines, the Propulsion Directorate is interested in reducing the TSFC of small turbines for use in UAVs and munitions. This thesis lays the groundwork for further study of TSFC reduction using ejectors. Follow on work could attempt to successfully unsteady the flow after the nozzle of the turbine to further increase thrust augmentation with the ejector.

II. Background and Theory

Overview

This chapter begins with a discussion that covers the basic theory and background of how ejectors create thrust. Following the primer on ejectors, related research which was particularly useful or possessed critical information for this investigation is discussed. The research has been grouped into categories by research type. Categories include cold source, hot source and analytical. This is followed by a brief analysis of the turbojet engine. All sections cover theory and operation as they apply to the research.

The Ejector

Regardless of geometry or configuration, ejectors operate by energizing a secondary flow with a primary source. Ejectors are devices which augment thrust by an energy exchange from the primary jet to the secondary jet. This exchange yields a thrust that is greater than the primary source alone and also has the complementary effect of making the entire assembly quieter. Using ejectors to augment thrust is not a new concept. The idea dates back at least to German research conducted during World War II [5]. A basic ejector system is shown in Figure 1. When considering ejectors for propulsion applications the primary source is usually of a smaller diameter and has a higher velocity stream.

This investigation and its discussion are considered in static conditions. Static conditions are defined such that the secondary flow stream is initially at rest prior to

being ingested by the ejector. Augmentation declines as the engine-ejector system airspeed increases [4].

Using basic sizing results from both unsteady and steady research an ejector was chosen for this research from a wide selection available at AFRL/PR. The diameter of the ejector was thirteen inches which gives a diameter ratio (D_{ej}/D_p) of 5.6. Length of the selected ejector was 65.5 in.

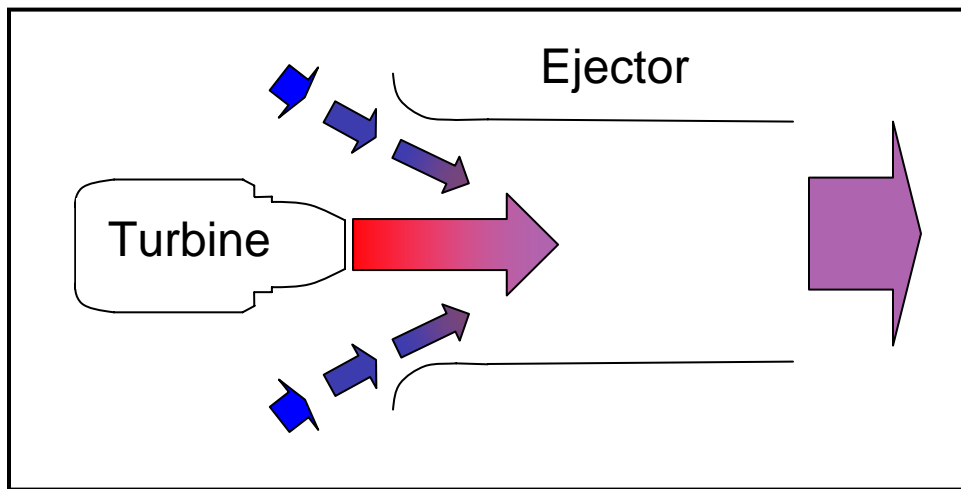


Figure 1. Basic ejector geometry

Ideal ejector analysis

An ideal analysis was accomplished to provide an upper bound on possible thrust augmentation. The ideal analysis helps show the effectiveness of different approaches on thrust augmentation. The ideal ejector behavior has been calculated using work accomplished by Heiser [6]. This work, which discusses basic thrust augmentation and then gives analytic solutions to various basic thrust augmenters, is formed using some assumptions. First, both the primary and secondary fluids exit the ejector at the same

velocity and in the thrust direction. Secondly, the flows exchange energy isentropically. The third and final assumption is that $U_a = 0$ or simply that the ejector is static.

Equations (1) through (17) from Heiser's analysis of an ideal ejector are listed below and are accompanied by an explanation of origin for each as needed. Figure 2 and Figure 3, show the naming convention and the control volume used during the equation derivations.

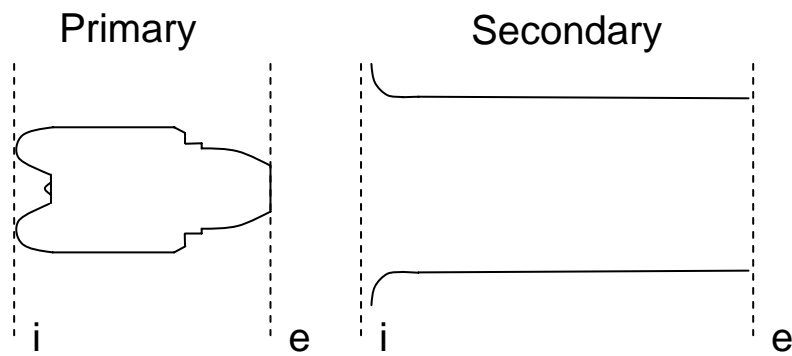


Figure 2. Engine-ejector naming schematic

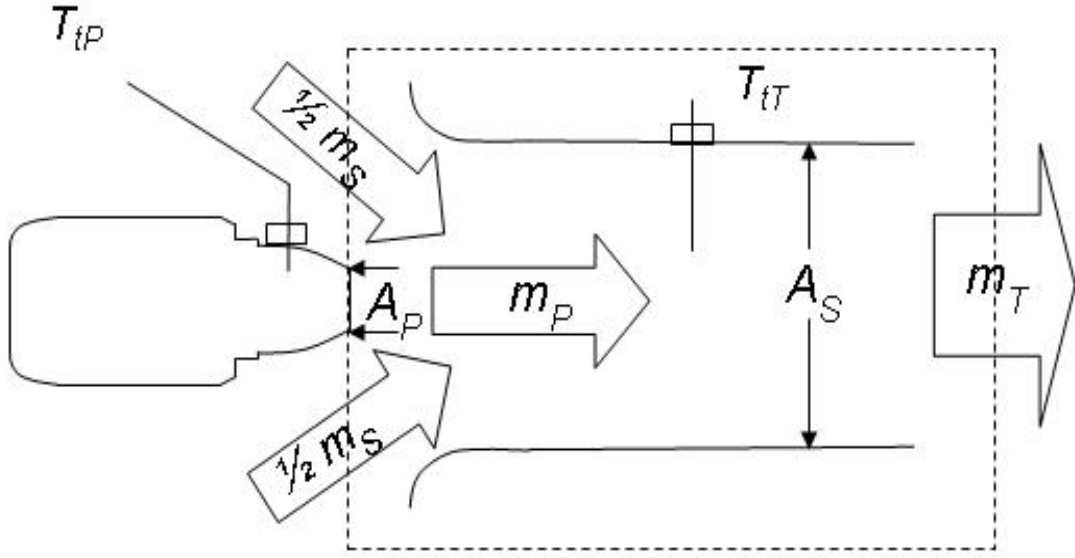


Figure 3. Engine-ejector control volume

Equations (1) and (2) are the Bernoulli equations [6]. The inlet conditions for both the primary and secondary flows are ambient conditions.

$$\frac{p_a}{\rho_p} = \frac{p_{Pi}}{\rho_p} + \frac{V_{Pi}^2}{2} \quad (1)$$

$$\frac{p_a}{\rho_s} = \frac{p_{Si}}{\rho_s} + \frac{V_{Si}^2}{2} \quad (2)$$

Define area ratio α as the primary area divided by the secondary area as shown in equation (3).

$$\alpha = \frac{A_p}{A_s} \quad (3)$$

When applied to the ejector control volume as seen in Figure 3, and combined with the area ratio, the Bernoulli equations become equations (4) and (5).

$$m_p = \alpha \sqrt{2\rho_p(P_0 - P_i)} \quad (4)$$

$$m_s = \sqrt{2\rho_s(P_a - P_i)} \quad (5)$$

The combination of equations (4) and (5) allows the elimination of P_i . The asterisk represents conditions after isentropic expansion to ambient conditions.

$$\alpha^2 = \frac{1}{\left(\frac{\rho_p V_p^*}{m_p}\right)^2 + \frac{\rho_p}{\rho_s} \left(\frac{m_s}{m_p}\right)^2} \quad (6)$$

Applying conservation of mass yields equation (7).

$$m_s + m_p = (\rho_s A_{pe} + \rho_s A_{se}) U_e \quad (7)$$

And now applying geometric constraints (total inlet area = exit area) yields equation (8).

$$A_{pe} + A_{se} = 1 + \alpha \quad (8)$$

A_{se} can be eliminated by combining equations (7) & (8).

$$m_s + m_p = U_e [\rho_s (1 + \alpha) + (\rho_p - \rho_s) A_{pe}] \quad (9)$$

Since $A_{p_e} = \frac{m_p}{\rho_p U_e}$ then equation (9) becomes equation (10).

$$m_s + \frac{\rho_s}{\rho_p} m_p = \rho_s U_e (1 + \alpha) \quad (10)$$

Defining thrust augmentation phi, as the total system thrust divided by the primary's thrust.

$$\phi = \frac{m_p U_{p_e} + m_s [U_{s_e} - U_a]}{m_p V_p^*} \quad (11)$$

Equation (10) and the definition of thrust augmentation are combined to eliminate U_e .

$$\phi = \frac{\left(1 + \frac{m_s}{m_p}\right) \left(\frac{\rho_s}{\rho_p} + \frac{m_s}{m_p}\right)}{\frac{\rho_s V_p^* (1 + \alpha)}{m_p}} \quad (12)$$

The conservation of momentum equation for the control volume gives equation (13).

$$(P_i - P_a)(1 + \alpha) = (m_p + m_s) U_e - \frac{m_p^2}{\alpha \rho_p} - \frac{m_s^2}{\rho_s} \quad (13)$$

Combining equations (4), (10) and (13) gives equation (14).

$$(P_0 - P_a)(1 + \alpha) = \frac{(m_s + m_p) \left(m_s + \frac{\rho_s}{\rho_p} m_p\right)}{\rho_s (1 + \alpha)} - \frac{m_p^2}{\alpha \rho_p} - \frac{m_s^2}{\rho_s} + \frac{m_p^2}{2 \rho_p \alpha^2} (1 + \alpha) \quad (14)$$

Rewriting equation (14), yields equation (15).

$$\frac{\rho_s V_p^* (1+\alpha)}{m_p} = \frac{\rho_s}{\rho_p} \sqrt{2 \left[\frac{\rho_p}{\rho_s} \left(1 + \frac{m_s}{m_p} \right) \left(\frac{\rho_s}{\rho_p} + \frac{m_s}{m_p} \right) - \frac{\rho_p}{\rho_s} (1+\alpha) \left(\frac{m_s}{m_p} \right)^2 + \frac{1-\alpha^2}{2\alpha^2} \right]} \quad (15)$$

Equations (6) and (15) can be combined to yield equation (16).

$$\alpha^3 \frac{\rho_p}{\rho_s} \left(\frac{m_s}{m_p} \right)^2 + \alpha \left[2 \frac{\rho_p}{\rho_s} \left(1 + \frac{m_s}{m_p} \right) \left(\frac{\rho_s}{\rho_p} + \frac{m_s}{m_p} \right) - \frac{\rho_p}{\rho_s} \left(\frac{m_s}{m_p} \right)^2 - 2 \right] - 2 = 0 \quad (16)$$

Equations (12) and (15) are combined to give (17) which is the final result.

$$\phi = \frac{\left(1 + \frac{m_s}{m_p} \right) \left(\frac{\rho_s}{\rho_p} + \frac{m_s}{m_p} \right)}{\frac{\rho_s}{\rho_p} \sqrt{2 \left[\frac{\rho_p}{\rho_s} \left(1 + \frac{m_s}{m_p} \right) \left(\frac{\rho_s}{\rho_p} + \frac{m_s}{m_p} \right) - \frac{\rho_p}{\rho_s} (1+\alpha) \left(\frac{m_s}{m_p} \right)^2 + \frac{1-\alpha^2}{2\alpha^2} \right]}} \quad (17)$$

Equation (17), when solved along with equation (16), gives the thrust augmentation available for an ideal ejector. The ϕ calculated serves as an upper bound value one can expect to achieve with static steady-flow ejectors. Equation (17) gives thrust augmentation for an ideal ejector as a function of the ratios of mass flow rates and the fluid densities.

Equation (18), a form of the energy equation, shows the physical mechanisms in which a particle can exchange energy. Thrust augmenting devices can be divided into two categories: ones that exchange net work or heat and ones that do neither [6].

$$\frac{Dh^o}{Dt} = \frac{1}{\rho} \frac{\partial p}{\partial t} + T \frac{Ds}{Dt} + \frac{1}{\rho} \bar{u} \bullet \bar{f} \quad (18)$$

Considering the first category, which describes steady flow, no net force is exerted on the fluids. Consequently augmentation is achieved by turbulent entrainment, which takes place in the shear layer between the primary and secondary flows. This entrainment results in higher mass flow rates (MFR) at slower, more propulsively efficient velocities. The third term on the right of equation (18) allows this mechanism by including the viscous and turbulent shear stresses.

Unsteady sources are the second category. With unsteady flow a net force is achieved through “the work of interface pressure forces.” This mechanism features a moving pressure interface which physically pushes the secondary flow [5]. The mechanism for augmentation is contained in the first term on the right of equation (18). This first term incorporates the flow work due to the pressure waves of the primary. The second term covers entropy transport and represents the thermal transport to or from the secondary flow and is a combination of the first and second laws of thermodynamics.

Steady flow source

The steady flow source is one which the thrust does not vary periodically with time. Gas turbines and rockets are examples of propulsive sources which emit a steady flow. To answer the question of how does the ejector produce thrust when driven by a steady source we must consider the first of Heiser’s [6] two categories from the energy equation discussion above. Thrust augmentation is achieved through turbulent entrainment where work and/or heat is exchanged. By making some basic assumptions such as incompressible flow and the secondary flow initially at rest, Heiser is able to

predict an ideal ϕ . He shows analytically that an ideal ejector's augmentation value is bounded between one and two ($1 \leq \phi \leq 2$).

Unsteady flow source

Unsteady flow sources generate thrust by emitting pressure waves which are periodic. Pulsed jets and PDEs are examples of unsteady source engines and differ only in the type of wave emitted. A PDE emits a detonation wave while the pulsed jet emits a deflagration wave. These waves differ significantly in their speed and strength or pressure difference. Augmentation is achieved through the work of one pressure wave physically pushing on the second. This is a non-dissipative and reversible process. The benefits in thrust augmentation of unsteady sourced ejectors have been known since at least World War II where they were demonstrated in German V-1 missiles, which were powered by a pulsejet engine [5]. Since at least 1961, when Lockwood [7] showed that unsteady flow is better at producing thrust than steady flow, the superior augmentation available from unsteady sources has been known.

Related Research

Due to the long history that ejectors enjoy there has been research conducted in almost every conceivable configuration of primary and secondary flow. In 1979, Porter and Squyers [8] presented a list of over 1600 publications relevant to ejectors. It is safe to say that this list would be much longer had it been published today. Since there is such a plethora of data on ejectors a few salient and/or helpful works have been grouped under each major category below.

Non-engine driven

Non-engine driven research is typified by small setups using compressed air as the primary source. This compressed air, sourced from large air compressors, may be preheated or not. Compressors typically provide steady flow, however this flow can be perturbed in some way to create unsteady flow. This unsteady flow is created many different ways, to include mechanical and aero acoustic. Each method has both positive and negative attributes. Non-engine driven setups are usually very clean, compact and repeatable.

Choutapalli, Krothapalli, and Lourenco [1] have shown peak augmentation numbers of at least 2.3 with the following ejector sizing parameters $L_{ej}/D_{ej} = 3$ and area ratio $(A_s/A_p) = 10$. These results were created using a mechanical chopper wheel to create an unsteady flow as well as an inline heater to raise the primary source temperature. Their unsteady results were compared with steady jet results and showed that unsteady produced much more augmentation than steady.

Choutapalli, Alkislal, Krothapalli, and Lourenco [2], state that thrust augmentation is a weak function of Mach number and that thrust increases linearly with frequency. The primary source was conditioned using a mechanical chopper wheel to create an unsteady flow and an inline heater to raise the temperature. Augmentation peaked at 1.85 at an area ratio of 11.

Paxson, Wernet and John [9] used an electrical speaker to create the primary unsteady source and go on to explain that the inverse Strouhal number, or formation number, is indeed a relevant parameter for predicting geometrically optimized ejector performance. This research achieved a peak augmentation of 1.7. Wilson [10] describes

the optimal geometry of the ejector for maximum augmentation when driven with a Hartmann-Sprenger tube, which is an unsteady source.

Engine driven

The results of an extensive literature search for engine driven research yielded papers that focused on pulsejet, PDE, or rocket engines. There is little or no published research on thrust augmenting ejectors powered by gas turbines. Fundamental differences exist in the way pulsejets and PDEs create thrust. The ignition of a fuel-air mixture can produce either a detonation or a deflagration wave. A detonation wave is a supersonic flame front sustained by compression waves from a trailing reaction zone. A deflagration wave is a subsonic flame front sustained by heat transfer produced in chemical reactions. Considering a PDE, the increase in density produced across a detonation wave will provide the momentum change to produce thrust, whereas the deflagration properties are not conducive to producing thrust. However, a pulsejet uses discrete deflagration events as the mechanism that produces thrust. After each deflagration there is a sudden rise in temperature and pressure which forces a rapid expansion of the gas which is then propelled out of the exhaust [11].

Pulsejet engine-ejector data go back over sixty years and focus on the original groundbreaking work or work as of late. The more recent work is a direct result in the current interest in PDEs. Pulsejets, which operate using resonance, are very sensitive to back pressure which is heavily influenced by an ejector. The fundamental differences between the way pulsejets, PDEs and gas turbines create thrust will result in different performance when driving their optimally sized ejector.

Using a pulsejet driver, Paxson, Wilson, and Dougherty [12] quantified the effects primary source geometry and downstream distances have on thrust augmentation. Geometric variations in length, diameter and inlet radius for the ejector were studied as well as driver cross-sectional shape. The downstream distance (X), which is the distance measured from the primary source exit to the secondary or ejector inlet, was also varied to determine its effects on augmentation. Peak augmentation was found to be 1.8. The authors also note “no proven theory of unsteady ejector performance appears to exist in the literature... neither does a consistent set of design criteria or scaling laws that would allow the construction of an effective ejector for an arbitrary pulsed flow.” Paxson [13] goes on to say that “although some experimental work has been done in the past to study thrust augmentation with unsteady ejectors, there is no proven theory by which optimal design parameters can be selected and an effective ejector constructed for a given pulsed flow.” Lockwood’s often cited 1961 work [7] showed that an unsteady flow is better at producing thrust than a steady one.

Allgood et al. [14] state that in general thrust augmentation was found to increase with ejector length. Their data from straight-walled ejectors was comparable with steady flow ejectors. However, their data from divergent-walled ejectors showed almost two times the augmentation. This increase was reported as due to the additional thrust surface the divergent geometry allowed. They went on to note that the ejector was sensitive to the axial position of the driver.

Wilson et al. [15] noted as others have that their thrust augmentation data showed two maxima one with the ejector downstream distance positive and one with it negative.

The peak augmentation was found to be at 20 Hz, while runs at 40 Hz gave lower values. A chart was presented showing their results as compared to others and included the effect of ejector nose radius.

Since engine driven research requires a much more complex setup, it tends to have fewer data points than the non-engine driven. This results in repeatability issues and collected data being influenced by conditions outside of the researcher's control.

Analytic

Heiser's work [6], in 1967, provides extensive discussions and equation sets describing ideal thrust augmentation and theoretical maximums given different basic assumptions. He details a fairly simple analysis for the ideal thrust augmentor as well as the ideal ejector. Petty [4] provides an analytical study to determine theoretical limits of non-static ejector thrust augmenters. Non-static entails both the engine and the ejector translating as though in flight. In addition to their comprehensive empirical ejector work Choutapalli, Alkisar, Krothapalli, and Lourenco [2], also provide an analytic overview which covers their work with unsteady sources.

The Gas Turbine Engine

The gas turbine is a rotary engine that extracts work from a flow of combustion gases. A simple gas turbine engine is composed of an upstream compressor coupled to a downstream expansion turbine with a combustion area in between. The following description details the ideal cycle. Air is ingested through the inlet and drawn into the compressor which increases the temperature and pressure of the air. The now hot and

pressurized air flows into the combustion chamber where fuel is burned. This burning reaction increases both the temperature and entropy of the air through a constant pressure process. The combustion products are then forced through a nozzle into the expansion turbine. The turbine extracts the work needed to power the compressor while the remaining flow passes towards the nozzle. The combustion products perform dual duty. Some of the products are used to power the compressor while the remaining are exhausted at high speed through a nozzle. The nozzle, by decreasing area, increases the flow velocity. This hot, high-speed stream serves as the propulsion source. Figure 4, shows the airflow path for the research engine, a JetCat P200.

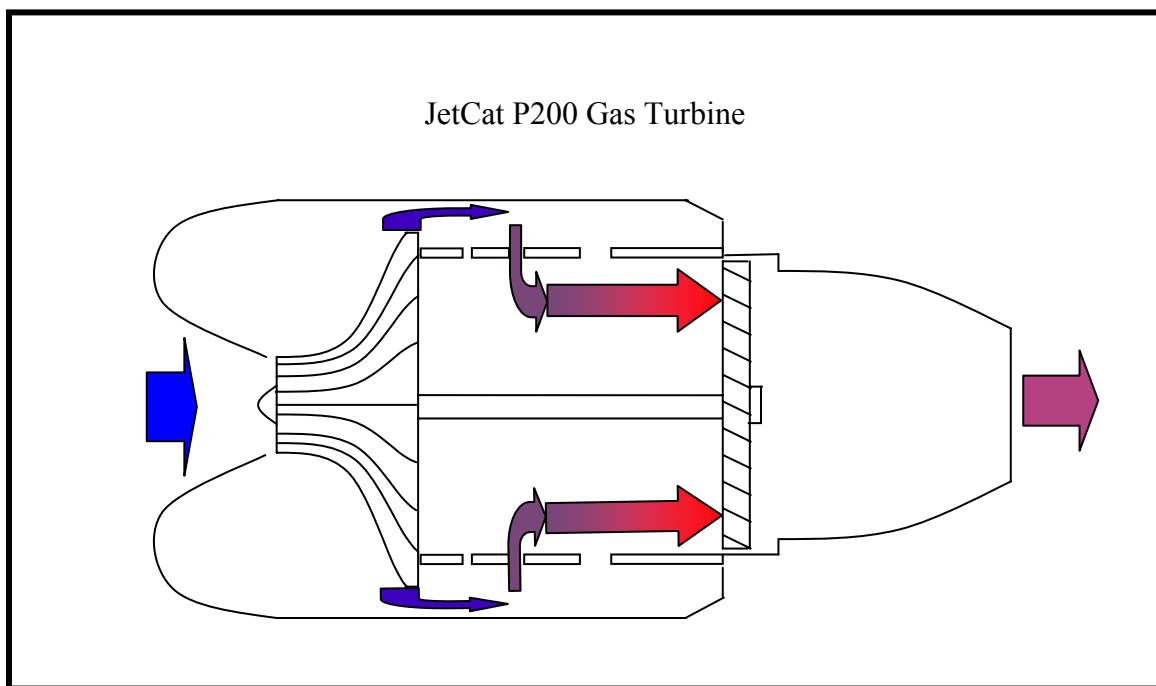


Figure 4. JetCat, gas turbine schematic

The gas turbine engine can be modeled using the Brayton cycle which is a constant pressure open system model. In order to analyze the engine as a cycle the

exhaust products are assumed to be ingested to create a closed system. The ideal P-v and T-s diagrams as well as the station numbering schematic which are used to describe the Brayton cycle are shown in Figure 5.

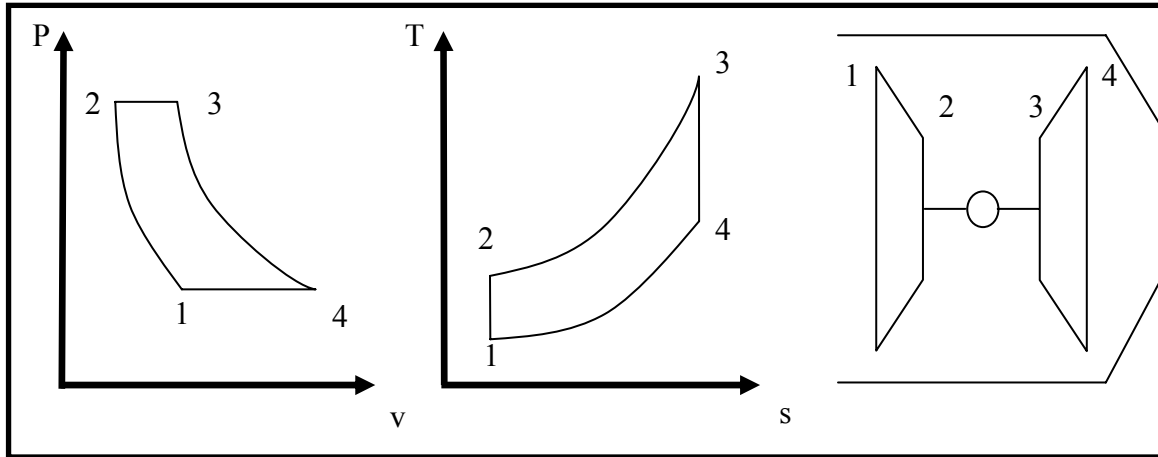


Figure 5. Ideal Brayton cycle P-v and T-s diagrams

Air begins at station one at the outside of the engine in front of the inlet. It flows through the inlet to the compressor face. The compressor then raises the pressure and temperature to station two. From two, the flow goes to the combustor where fuel is added and combustion takes place. A good combustor design is one that can raise the temperature, entropy and specific volume of the flow with minimal pressure variation. Combustion products are now directed towards station three. Station three begins immediately upstream of the turbine where the flow is forced to expand and subsequently cool as it passes through the turbine to station four.

Chapter Summary

Details of an extensive literature search provided a historical and current view of research efforts and the main focus areas. The concept of using an ejector to augment thrust is not a new idea. Ejector's history can be traced back to at least WWII where the Germans found unanticipated results when using an ejector with the pulsejet. Much analytic work has been done to show the upper bound or ideal ejector's performance window. Discussion followed regarding the basic application and use of the JetCat P200 as the primary source to drive the research ejector. A primer in basic ejector and gas turbine theory was given in an effort to clarify terminology and specifics regarding basic operation of each.

III. Materials and Methodology

Overview

This chapter will discuss the materials and methods by which this research was conducted. First, capabilities of the research facility to include the thrust stand and control room are covered. Next, a description of the engine system and subsystems is given. To conclude the chapter an explanation of the test setup and procedures is detailed.

D-Bay Facility

The research was performed at Wright Patterson Air Force Base, Ohio, Building 71A, D-Bay which is known as the Pulsed Detonation Research Test Facility. The PDE facility is managed and sponsored by the Air Force Research Laboratory, Propulsion Directorate, Turbine Engine Division, Combustion Sciences Branch (AFRL/PRTC) in conjunction with the Innovative Scientific Solutions, Inc. (ISSI) contractor.

The PDE facility is a 21,200 m³ (748,670 ft³) explosion proof test cell originally intended for turbojet testing. The facility contains a 267,000 N (60,024 lbf) turbojet thrust stand. The facility also contains workspace and tools to perform maintenance and minor part fabrication. The fuel and control rooms are separated from each other and the test cell by two-foot thick, steel reinforced, concrete walls. The JP-8 and oil mix is stored and prepped in the fuel room. The control room is used for engine control, data collection and real time monitoring through closed circuit cameras. The engine is operated from a dedicated computer running a control panel generated by JetCat

software. The fuel room and engine operation can be monitored and recorded from the control room cell through a closed circuit television.

The research facility is spacious enough to house multiple projects at once while still allowing complete access to necessary systems. The engine thrust stand where the PDE research takes place is built to be modular, which allows multiple projects to test in series. As one project is taking data another can be working to refine the test setup. The research engine and ejector system are mounted to the thrust stand and controlled remotely. All required data is collected using either the engine's Engine Control Unit (ECU) internal storage capability or the PC which hosts the thrust stand control via LabVIEW.

Air Supply System

Fuel flow is controlled by a pneumatic fuel valve. Air for the pneumatic fuel valve is provided by an Ingersoll-Rand Pac Air Compressor (Model# PA 300V) capable of producing 40 m³/min (1412 ft³/min) rated to 6.8 atm (100 psi) and stored in a 4.5m³ (159 ft³) receiver tank (Serial# 10894, Buckeye Fabrication Co.). Due to size and noise levels, the compressor and receiver tank are stored in a separate room in D-Bay known as the compressor room. The air is routed out of the compressor room into the test cell under the test stand.

Engine Thrust Stand

The thrust stand is a damped engine thrust stand mounted on top of a large scale static thrust stand. The damped engine stand is thrust rated from 3 to 1000 lbf and is

accurate to ± 1 lbf. Owing to its development for PDEs, the stand was designed to measure the time-averaged thrust of dynamic engines. The test item is rigidly affixed to the cart which has linear bearings riding on a pair of low-friction rails. The cart is weakly damped by load spring(s) which prevent resonance effects. The stand is oscillated using a pneumatic actuator to eliminate or reduce static and Coulomb friction effects. Since this is a known periodic force it can be differenced out of the final thrust measurements.

Calibration of the stand is accomplished using metal weights which are hung from a wire rope to affect a displacement. Weights, in five pound increments, are placed on the calibration hanger and the displacement is read from the linear displacement sensor as can be seen in Figure 6. The process of adding weights is continued until the stand has been calibrated in the thrust range of interest. For this research the stand was calibrated from fifteen to sixty pounds. The travel length of the thrust stand on its linear bearings is limited by the linear displacement sensor. To stop the sensor from bottoming out there must be some offset weight on the stand. An offset weight of fifteen pounds was used for all thrust measurements.

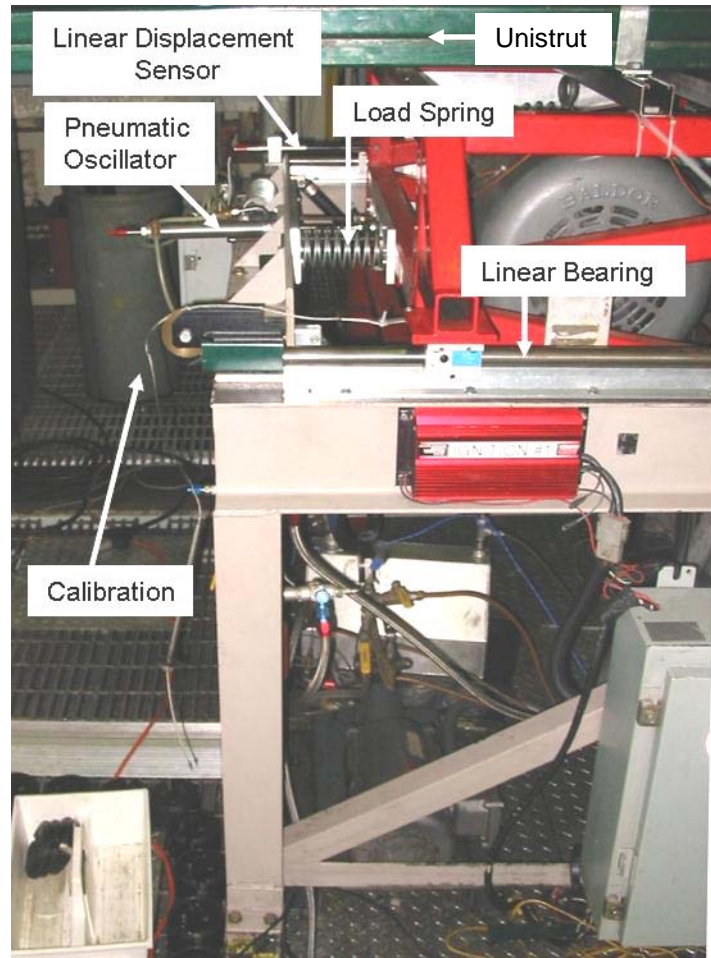


Figure 6. D-bay thrust stand diagram

Instrumentation

Instrumentation varied for each of the tests performed. At a minimum each setup consisted of the JetCat engine instrumentation and data acquired from the D-bay data acquisition system. The JetCat ECU stores roughly twenty minutes of data to non-volatile memory which is downloaded at the conclusion of each test. The D-bay data acquisition system supplanted the ECU by collecting test environment data and most importantly thrust data. Both sets of data, once collected, were compiled by hand.

D-Bay Instrumentation

The PC which hosts the LabVIEW program not only operated the test cell but also collected the actual test time, barometric pressure, test cell temperature and thrust for each run. When configured, engine nozzle back pressure and multiple temperatures were also measured using this PC.

Engine Instrumentation

The JetCat ECU is capable of gathering and displaying eleven different data fields. Of these eleven fields system time, Exhaust Gas Temperature (EGT), actual RPM, engine state and both pump and battery voltages were retained and analyzed. The remaining fields are only pertinent to the engine while in-flight and remotely controlled.

Engine

The engine used for this research, as seen in Figure 7, is a commercially available turbojet engine used in the model aircraft industry. The JetCat P200 is a single spool non-afterburning turbojet which uses an axial turbine to drive the centrifugal compressor. The engine is manufacturer rated to produce 45 lbf at 112,000 RPM. Further published parameters can be seen in Table 1.

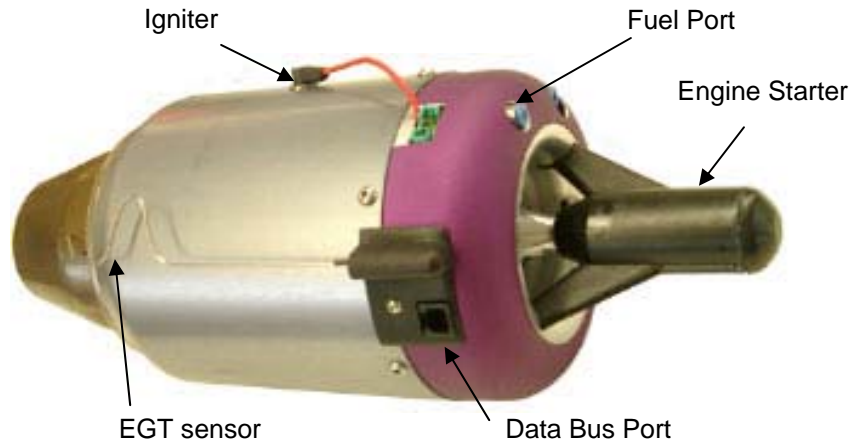


Figure 7. JetCat P200 turbine

Table 1. JetCat P200 published and measured data

	Published	Measured
Idle RPM (1/min)	33000	33000
Max RPM (1/min)	112000	112000
idle thrust (lbf)	2	2.0
max thrust (lbf)	45	47.5
EGT (F)	1328	1344.0
Pressure ratio	4	--
Mass flow rate (lbm/s)	0.99	--
Exhaust Gas Velocity (ft/s)	1604	--
Power output (hp)	72.15	--
fuel consumption max (gal/min)	0.193	0.187
fuel consumption idle (gal/min)	0.034	0.034
SFC @ 100% $\left(\frac{\text{lbm}}{\text{hr} * \text{lbf}} \right)$	1.54	1.42
weight (lbm)	5.2	--
diameter (in)	5.2	--
length (in)	14.0	--

Operation and maintenance

The JetCat turbine has been built to be simple and reliable. Once fuel and charged batteries are connected, the engine can be started. Using the Jet-tronic software (version 1.0.59) user interface, as seen in Figure 8, the engine can be controlled. The engine Graphical User Interface (GUI) commands the engine to run using the control labeled Aux in Figure 8. The engine will go through an automated startup sequence where the burner is preheated for five seconds, then the starter motor spins the turbine to ignition RPM (5,000 RPM). After five seconds the engine ignition begins by injecting fuel into the ceramic igniter. When the engine lights, the RPM is advanced and the idle RPM is established at 32,000. Once the ECU has established the idle RPM, control of the engine is returned to the user. Throttle inputs correspond to RPM percentage where idle is zero and 112,000 RPM is 100%. The vertical slider labeled throttle, as seen on the left of Figure 8, allows the operator to input the percentage RPM desired. Unplanned maintenance can be accomplished at any time by returning the engine to JetCat. The only required maintenance of the engine occurs after twenty five hours of engine operation. At twenty five hours of operation the turbine needs to be returned to the manufacturer for main shaft bearing replacement. Scheduled maintenance should also include keeping the exterior case and starter hub clean and degreased.

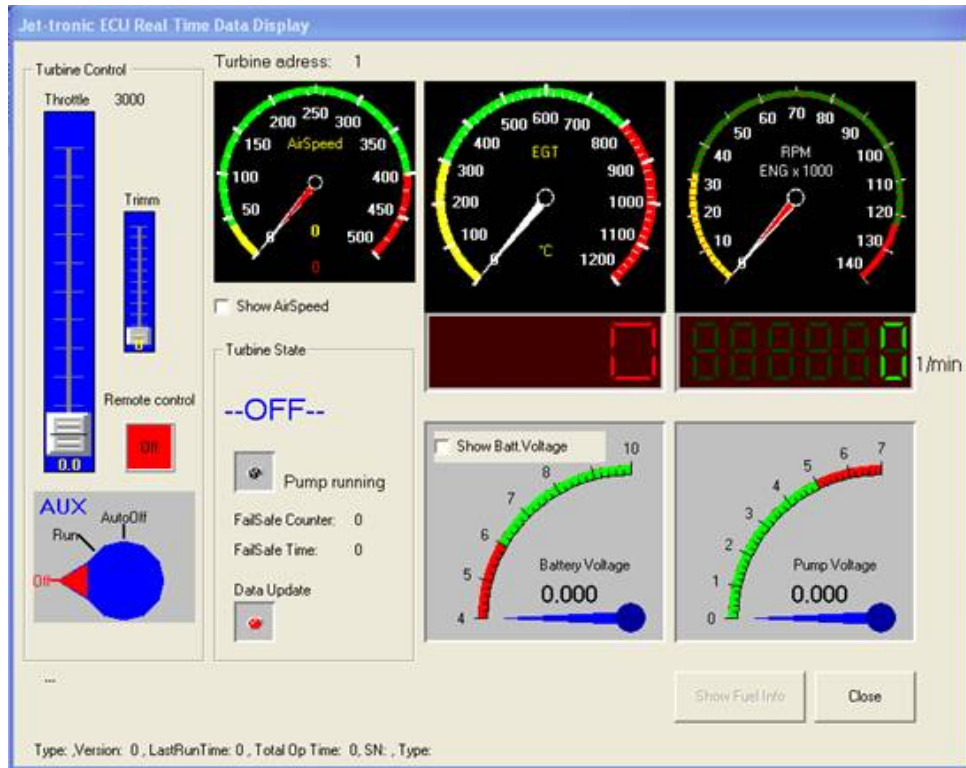


Figure 8. JetCat engine control software GUI

Engine Control System

The central component of the engine control system is a Hitachi H8 microcontroller that resides in the ECU. While the ECU's primary task is controlling the engine, it can also store key parameters in its non-volatile memory. The ECU automatically collects: system time, spool RPM, commanded RPM, exhaust gas temperature, fuel pump voltage, engine control state, throttle stick position, and battery pack voltage as well as other parameters not used during the research. Using spool RPM and fuel pump voltage, the ECU maintains the commanded throttle percentage. The two electric solenoids located in the fuel lines allow the ECU to execute commanded startups and shutdowns. An RS-232 interface connects the ECU to a laptop computer in the

control room. This laptop issues commands to the engine, shows real-time critical engine parameters and retrieves the data stored on the ECU after the run.

Engine Electrical System

The P200 engine electronics are designed to operate on 7.2V DC due to their model aviation heritage. Two 2400mAh NiCd batteries in parallel are the main source of power used to run the ECU which apportions energy as needed to the engine starter, fuel pump, and fuel solenoids. A DC power supply, also in parallel, augments and doubles as a battery charger during off-peak demand times. The electrical system can be seen in Figure 9.

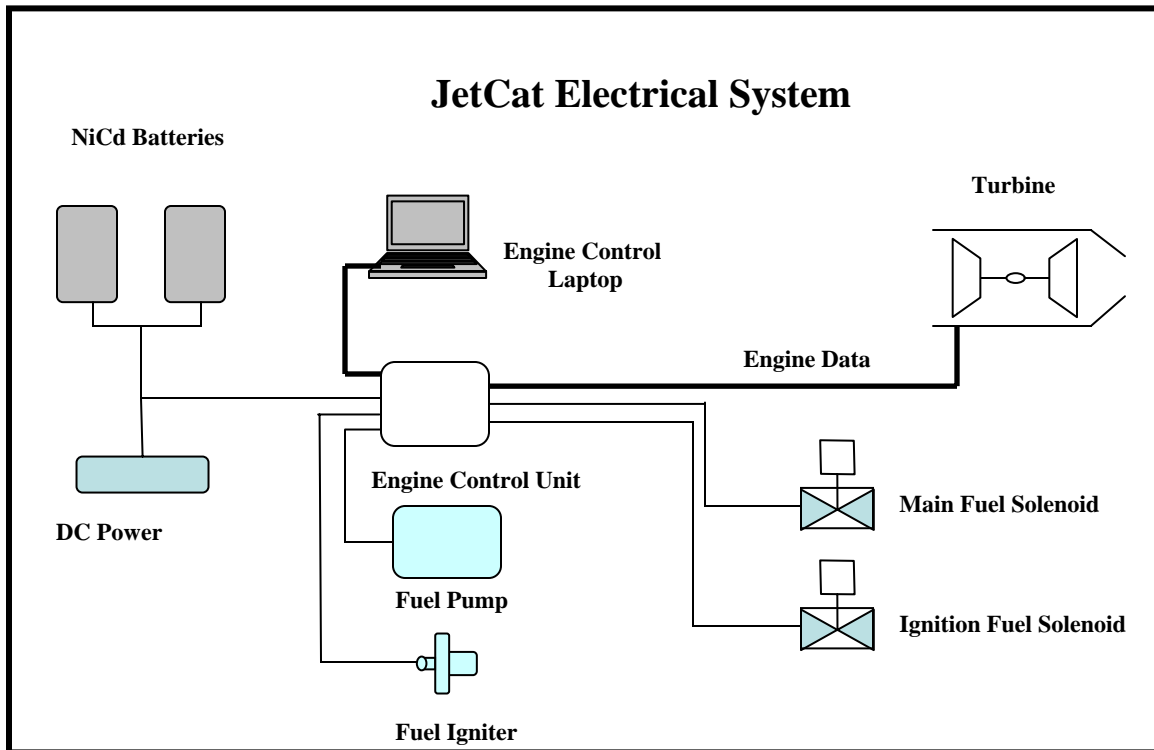


Figure 9. JetCat electrical system

Engine Fuel System

Fuel for the P200 is JP-8 with a five percent mixture of synthetic turbine oil, in this case AeroShell 500 turbine oil. The engine requires the fuel-oil mix for proper bearing lubrication and corrosion protection. A gravity fuel feed system was adopted due to its simplicity and ease of use. When the pneumatic fuel valve, which is actuated from the control room, is opened fuel is allowed to reach the fuel pump as in Figure 10.

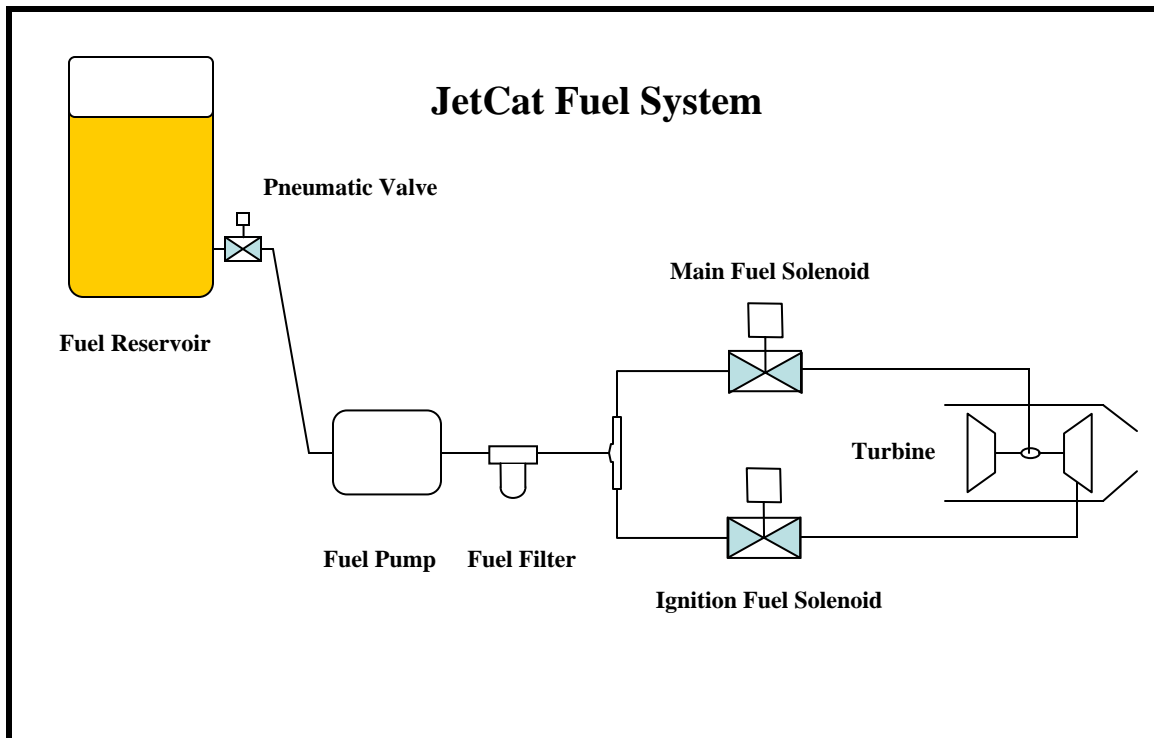


Figure 10. JetCat fuel system

Test Procedures

Before testing, the JP-8 and turbine oil are mixed in a five gallon fuel container in the fuel room. The fuel container, after mixing, is moved to the test cell where it is located above the engine thrust stand. The fuel and air lines are connected to the container. The D-bay compressor which supplies air for the thrust stand oscillator is also used to power the pneumatic fuel valve.

From the control room, the thrust stand oscillator and fuel systems are actuated using a LabVIEW interface. The thrust stand is allowed to oscillate for roughly thirty minutes to allow the linear bearings to oil and set in. While the stand is oscillating the engine fuel lines are bled of air, the fuel filter checked and the thrust stand calibrated.

Upon completion of the before-test items, testing can begin. The Jet-tronic software is used to control the engine and collect important engine parameters during testing. The software is loaded on the laptop which is connected to the ECU via an RS-232 interface cable. When the software is started the connection to the ECU is established. Once the automated start sequence has completed, control of the engine is turned over to the user. Upon completion of the data run the engine is commanded to shutdown. The turbine has two shutdown procedures that can be commanded either manual off or auto off. Manual off is reserved for emergencies as it immediately stops fuel flow. Auto off is the normal method for turbine shutdown. When commanded to auto off the turbine will stabilize to the most thermally efficient speed (around 55,000 RPM) to allow the engine to cool. It will maintain this speed for about six seconds before shutting down. After the spool has stopped rotating the starter motor will engage periodically to draw in cool air until the exhaust gas temperature has dropped below 100 degrees Celsius. Once the automated shutdown sequence has completed, run data can be retrieved using the engine control laptop.

All attempts were made to collect each data series in one day. After the data were collected the baseline configuration (engine alone) was run to get the thrust data. Each data series augmentation values are calculated using the baseline engine thrust for that day. This was done in an attempt to mitigate large changes in atmospheric pressure, test cell temperature, and humidity, which can change significantly from day to day.

Test Setup

The research setup was hand built using Unistrut, which is a system comprised of spring nuts and bolts connected to a continuous slotted channel. Unistrut was chosen due to its current usage and availability in D-bay and its ease of use. The engine thrust stand is fitted with Unistrut top rails which serve as the anchor point for the turbine ejector system. The system was designed to be both scalable and modular. Scalability was built in to allow the engine to ejector distance (X) to be adjusted simply. The modularity was needed since the turbine cannot be exposed to the environment of an operating PDE due to its extreme harshness. The shocks emitted by the PDE create vibrations that could high cycle fatigue the aluminum components in the engine. Since testing was done during on-going PDE research the assembly needed to be modular to allow ease of assembly/disassembly.

Chapter Summary

An introduction was given to the research materials and methodology used to collect the data. The D-bay facility is the perfect location to conduct research on propulsion systems, specifically engines that create an adverse noise environment. Since the research engine's controls are almost completely self-sufficient, little was required from the engine stand or facility. The engine was controlled remotely and all data were acquired using either the non-volatile memory on the engine ECU or using the PC which hosts the thrust stand controls and data acquisition system.

IV. Results and Discussion

Overview

Ejector thrust augmentation results were collected in three series. Series one consisted of the engine and ejector. Series two used the same ejector and turbine with the addition of a collector tube. Series three included a metal wheel and collector system which mechanically chopped the flow to create unsteady flow. The engine was set to exhaust into the center of the ejector, this axisymmetric configuration was used for all data series. Figure 11 summarizes averaged augmentation results and is presented to allow the user an overview of the results of series one and two. Next, the methods and equations used to obtain the data needed to calculate the ideal case are discussed. Following the actual data and ideal curves from all three data series are presented. Included with this are discussions and graphs of key results.

Figure 11 shows time-averaged thrust augmentation as a function of downstream ejector distance and also engine throttle position. Of interest to note is that the peak augmentation for series one did not occur at maximum throttle. The peak appears at an engine throttle setting of 80%. This finding illustrates an area for improvement, if peak augmentation is desired. An ejector sized to maximize thrust augmentation at 100% rather than 80% would allow for the greatest overall system thrust.

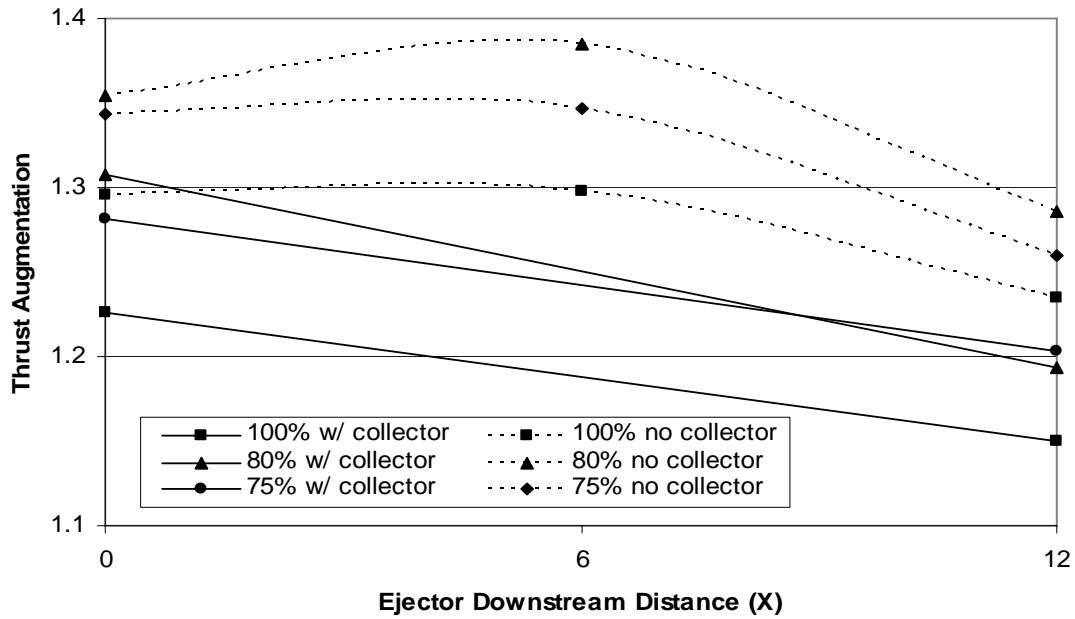


Figure 11. Variation of ϕ with downstream distance and throttle percentage

Modeling the turbine

Using the Oates's companion software [16] the JetCat engine was modeled to provide exhaust velocity, temperature and mass flow rate at different throttle settings.

The parameters input into the software can be seen in Table 2.

Table 2. Oates software inputs

Fuel Heating Value	19500 Btu/lbm
Turbine Gas Properties	$C_{p_t}=0.297$; $\gamma_t = 1.3$
Compressor Gas Properties	$C_{p_c}=0.24$; $\gamma_c = 1.4$
Component Total Pressure Ratios	$\pi_{D_{max}}=0.98$; $\pi_B=0.94$; $\pi_N=0.98$
Turbomachinery Polytropic Efficiencies	$e_c= 0.74$; $e_t= 0.815$
Combustion and Mechanical Efficiencies	$\eta_B=0.98$; $\eta_S=0.99$
Geometric design parameters	Exit nozzle = convergent MFR _{air} =1lbm/s Compressor Press Ratio = 4

Using the software the engine was modeled as a fixed area turbojet using the engine off-design performance program. Parameters were chosen based on appropriate figures of merit listed in Mattingly's books [17, 18]. Using measured and published data, the model was refined until its performance closely mirrored the actual turbine as seen in Table 3.

Table 3. Oates modeled engine results compared with known values

	Published or Measured	Modeled
Exhaust Velocity (ft/s)	1600	1650
Fuel Flow Rate (lbm/hr)	68	79
Thrust (lbf)	47.5	52
Tt9 (R)	1344	1340
Mass Flow Rate (lbm/s)	0.99	1

Table 3 contains values for the engine at 100%. To obtain values at 80%, 75% and 50% different values of T_{t4} were tried until the model closely matched the observed performance at each throttle setting. Once the engine model matched the observed values the data were recorded for use in future calculations.

A few basic calculations must be performed in order to allow one to compare the actual engine performance to the model predicted performance. The Oates [16] software engine model calculates the uninstalled thrust of the engine. That is the thrust generated by the engine without any aerodynamic shell. Additive drag is the result of the inlet geometry of this shell. This value of uninstalled thrust is higher than the actual thrust since the additive drag (D_{add}) has not been included. To calculate installed thrust, one must subtract D_{add} value from the Oates predicted thrust. The equation used to compute

the additive drag can be found in Oates's book and is shown below as equation (19).

Figure 12 shows the station numbering scheme used in equation (19).

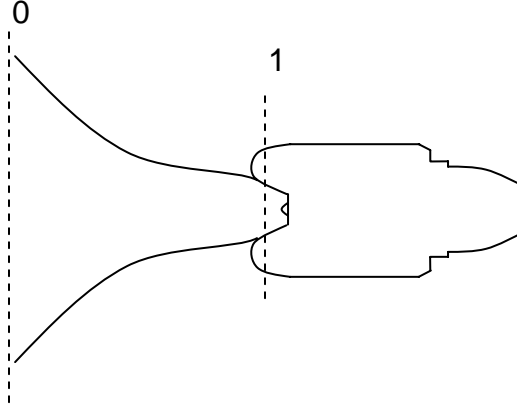


Figure 12. Inlet control volume for additive drag

$$D_{add} = m_1(V_1 - V_0) + A_1(P_1 - P_0) \quad (19)$$

$$\rho_0 = \frac{P_0}{RT_0} \quad (20)$$

Since the Mach number of the flow is less than 0.3 the flow can be considered incompressible thus $\rho_0 = \rho_1$. Also since the flow starts at rest, $V_0=0$. Using the turbine model for MFR, equation (22) for density and the turbine inlet area of 11 square inches will give velocity as in equation (21).

$$V_1 \approx \frac{m_0}{\rho_0 A_1} \quad (21)$$

Now, by having fluid density and velocity equation (19) becomes equation (22).

$$D_{add} = m_1(V_1) + A_1 \left(-\frac{\rho_1 V_1^2}{2} \right) \quad (22)$$

For this engine the D_{add} was calculated to be roughly 2.7 lbf at 100% throttle. The temperature measured at the entrance to the nozzle can be assumed to be T_{t5} . Equation (23), which can be found in Oates, allows the close approximation of the turbine inlet temperature, T_{t4} using the measured temperature at the nozzle entrance, the published compressor pressure ratio and the figures of merit from Table 2.

$$T_{t4} = T_{t5} \left(\pi_c \right)^{\frac{\gamma_t - 1}{\gamma_t e_t}} \quad (23)$$

Solving equation (23) gives T_{t4} as equal to 2100 R. The T_{t4} , calculated D_{add} , and the values listed in Table 2 give the needed inputs for the engine model to be refined in the Oates software.

Calculation of secondary flow conditions

Rather than acquiring data to characterize the secondary flow an analytical approach was utilized. With a simple control volume analysis the secondary flow parameters can be calculated using known parameters. Total temperature at nozzle exit and mid-tube on the ejector were measured using type J iron-constantan thermocouples. The temperature and the mass flow rate of the primary are used to calculate the mass flow rate of the secondary stream. By assuming a calorically perfect gas and an adiabatic ejector the analysis reduces to a simple series of equations. Starting with conservation of

energy equation (24) and applying it to the control volume as seen in Figure 3 a basic equation can be derived to relate primary mass flow rate to secondary mass flow rate.

$$E_p + E_s = E_T \quad (24)$$

$$E = mC_pT_t \quad (25)$$

By relating the energy equation to the control volume as shown in Figure 3, a basic equation can be derived to relate primary mass flow rate to secondary mass flow rate. This generates equation (26).

$$m_p C_{pP} T_{tP} + m_s C_{pS} T_{tS} = m_T C_{pT} T_{tT} \quad (26)$$

Since the secondary flow is initially at ambient conditions and with C_p assumed constant equation (26) simplifies to equation (27).

$$m_p T_{tP} + m_s T_{tS} = m_T T_{tT} \quad (27)$$

Using continuity the total mass is the sum of its parts and solving for m_s .

$$m_s = \frac{m_p (T_{tP} - T_{tT})}{(T_{tT} - T_{tS})} \quad (28)$$

By solving equation (28), m_s can be found. Assuming a perfect gas gives equation (29).

$$\rho = \frac{P}{RT} \quad (29)$$

Since the secondary stream begins at ambient conditions equation (29) becomes (30).

$$\rho_s = \frac{P_a}{RT_a} \quad (30)$$

In order to obtain the mass flow rate and density of the exhaust stream the engine was operated at different throttle settings using modeling software. This gave sufficient data to calculate, using equations (24) - (28), and the secondary mass flow rate. Secondary flow density can be obtained from equation (30). These two results can be used in equations (16) and (17) of the ideal ejector analysis to calculate ideal ejector thrust augmentation.

Data Series One

Data series one used the exhaust from the nozzle to power the ejector directly as can be seen in Figure 13. For each run the distance from the engine exit plane to the inlet plane of the ejector was increased from (X=0, 6 and 12 inches). This was followed by a baseline run without the ejector.

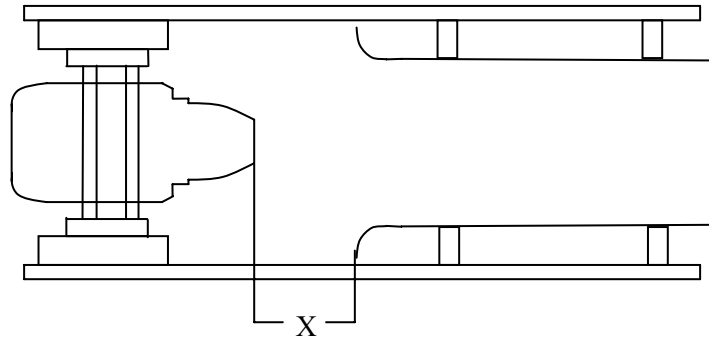


Figure 13. Series one test setup

Figure 14, Figure 15 and Figure 16 are included to give the reader an overall understanding of the engine-ejector configuration.

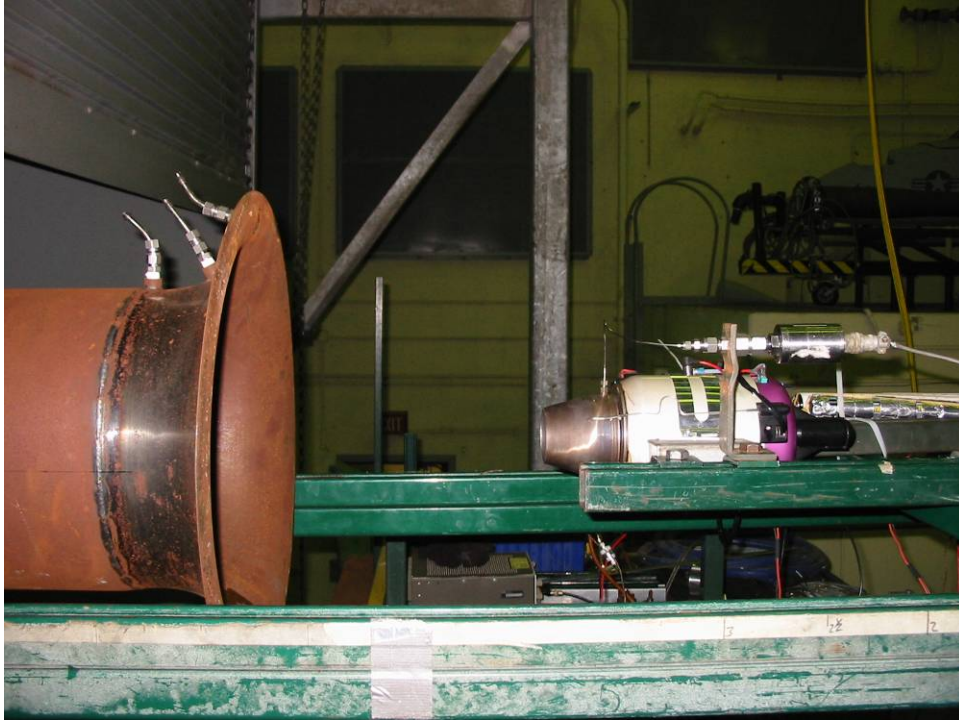


Figure 14. Series one, X=12" side view

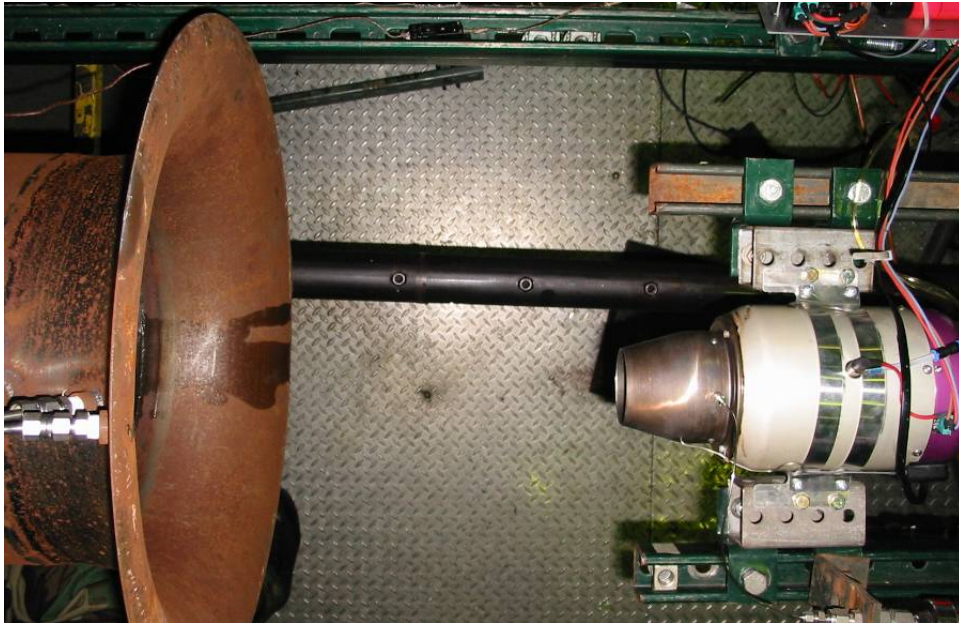


Figure 15. Series one, X=12" top view



Figure 16. Series one, engine baseline

Figure 17 compares the actual augmentation at different ejector distances with a theoretical value obtained using Heiser's [6] analytical work. It can be seen that the actual values fall short of the analytically predicted values. The lines depicting Heiser's ideal analysis portray ideal ejectors and do not take into consideration geometry of the test setup or compressibility of the fluid. Both the on-plane and the $X=6''$ configuration show good correlation with one another. They entrain similar secondary mass flow rates and behave near ideal. The $X=12''$ case does not. To correct this one must modify the primary MFR to account for the increased mass resulting from the jet mixing with the ambient air prior to entering the ejector. The apparent poor performance at $X=12''$ is due to two interconnected reasons. Once the primary flow leaves the exit plane of the nozzle it begins to mix and expand. This effect becomes very pronounced at twelve inches where the flow stream has had ample time to mix and entrain more mass. The other

contributing factor is that the energy equation used to solve for the secondary flow uses total temperatures to relate mass flow rates. As the X distance grows the jet exhaust is allowed to mix with the ambient air which causes the outside of the jet to cool. This cooling coupled with the larger primary MFR cause the augmentation to degrade and the ideal prediction to breakdown.

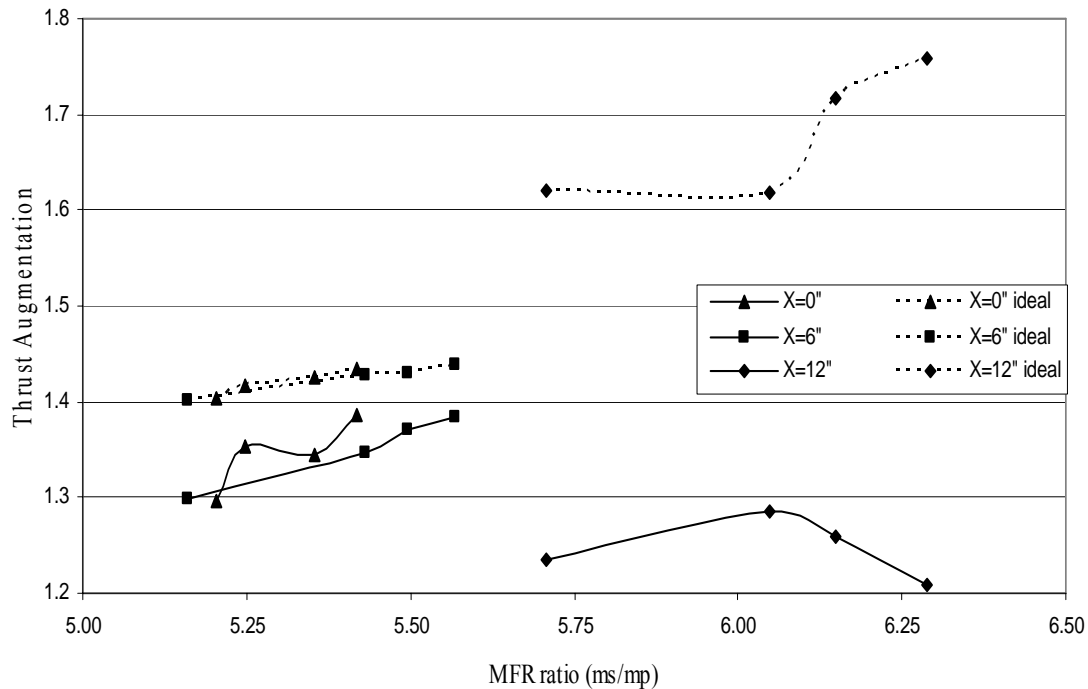


Figure 17. Comparison of ϕ for actual and ideal ejector system

As can be seen in Figure 18 there is a peak augmentation value attainable for each X distance of ejector spacing. Engine throttle at 80% yields this peak or greatest augmentation value. A diminishing return can be shown in the ideal case as seen by the Heiser lines. Stated another way thrust augmentation does not continue to increase as throttle is increased past 80%.

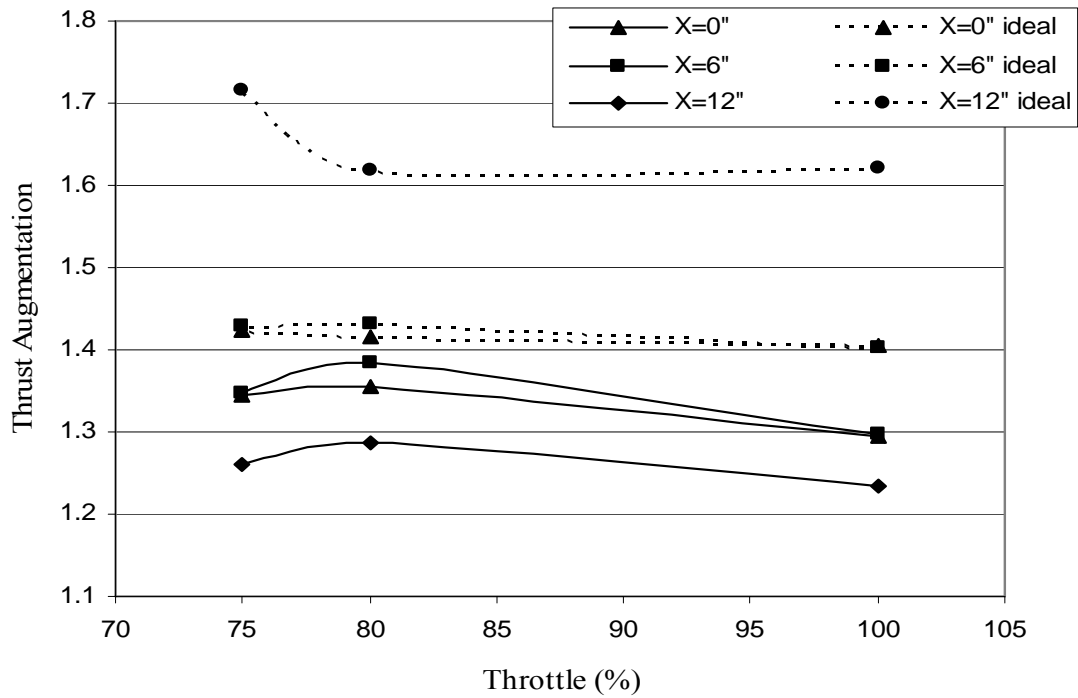


Figure 18. Effect of X distance on ϕ for both actual and ideal ejector systems

Data Series Two

Data series two used the same engine and ejector; however after the turbine exhaust a 14" long, 3" diameter stainless steel pipe or collector was inserted. This was done for two reasons. First, since data series three would use the collector in conjunction with the chopper wheel a characterization of the effects on thrust was needed. Second, in an effort to determine if the engine nacelle had any effect on the ejector's inlet flow the collector was added. Data were collected at two different downstream distances (X=0" and 12").

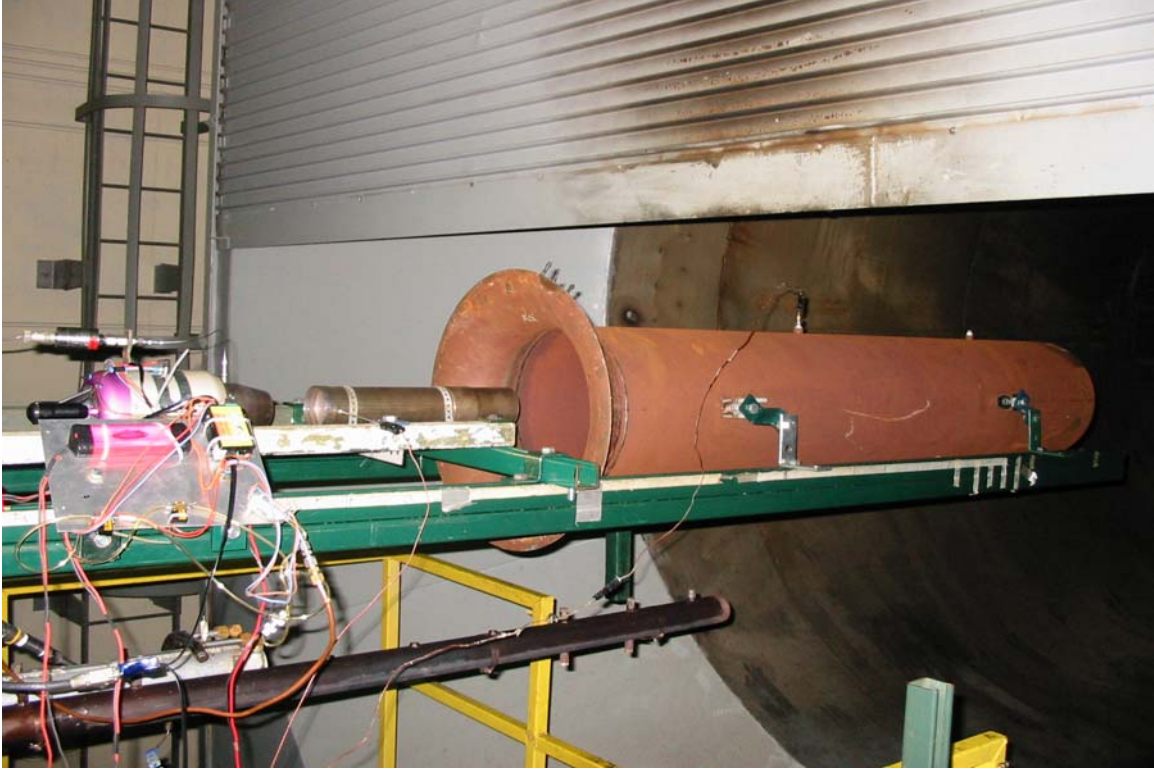


Figure 19. Series two $X=0''$ side view

Figure 20 summarizes the results by X distance. Comparison of Figure 18 with Figure 20 will show that the collector had an overall deleterious effect on thrust augmentation. The collector tube cost four percent at an X distance of zero inches and ten percent at $X=12''$.

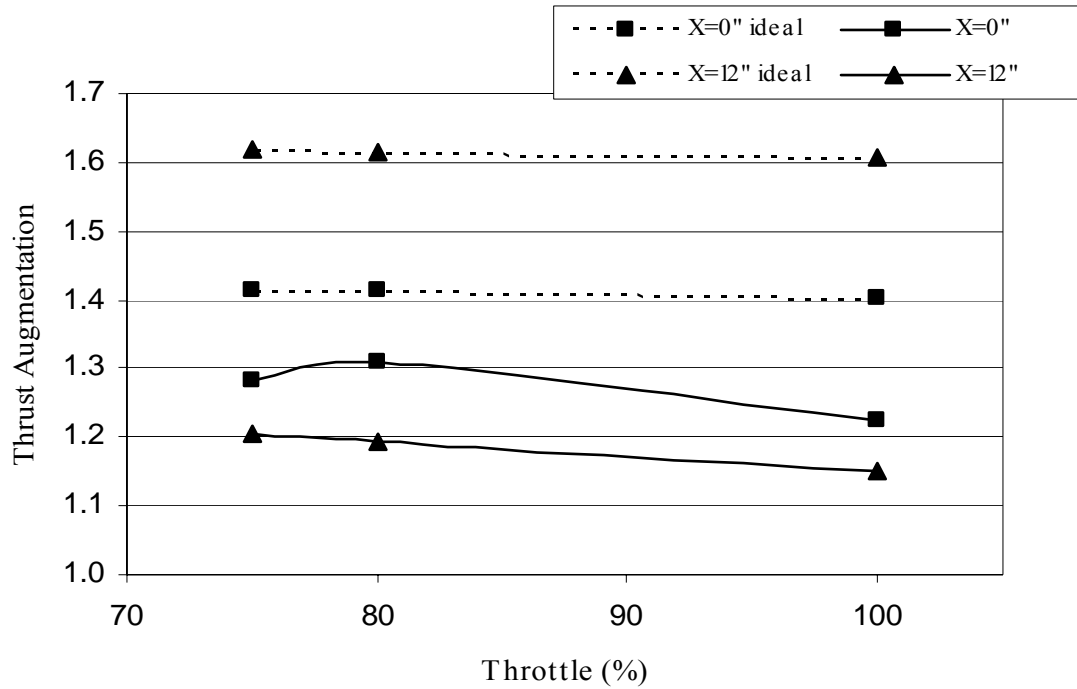


Figure 20. Effect of X distance on ϕ for engine, collector and ejector system

Figure 21 shows much as Figure 17 did that an X distance of 12" does not produce good augmentation and this is only exacerbated by the collector tube. The poor augmentation capability and the drag/weight penalty resulting from the physical geometry of the X=12" system do not make it a good candidate for further analysis.

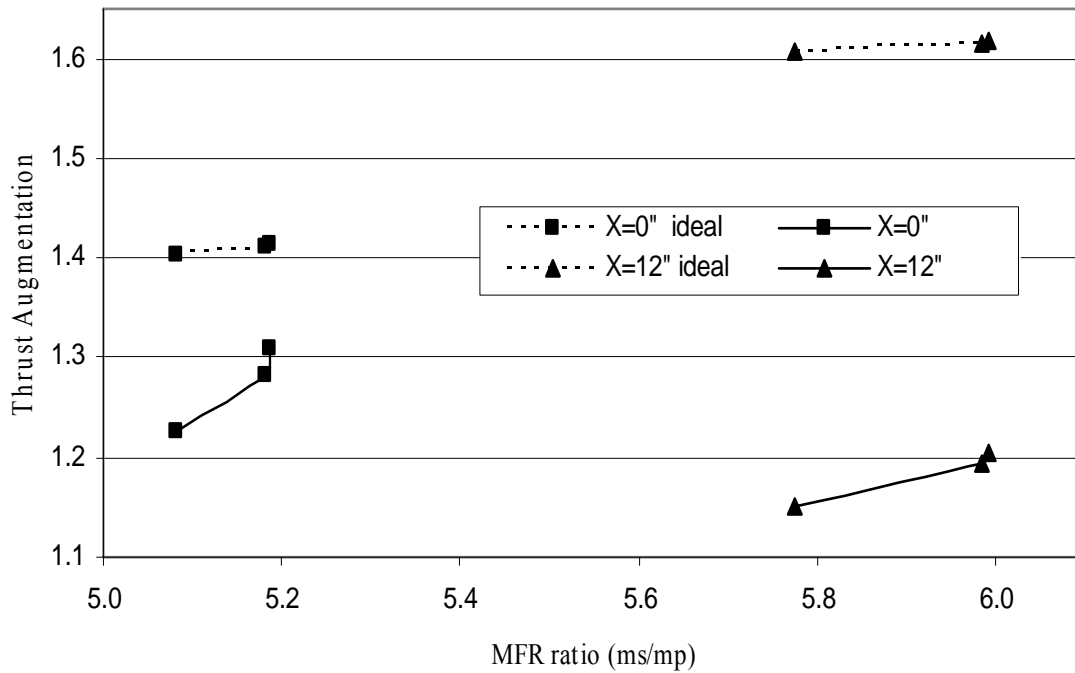


Figure 21. Thrust augmentation variation with MFR ratio with collector tube

Data Series Three

This data series used the same engine and ejector system but incorporated a mechanical flow disruptor and a collector. The collector was incorporated in an effort to return the flow after chopping to a more axisymmetric state prior to it entering the ejector. This system was investigated in an effort to explore possible methods of creating an unsteady source using a gas turbine.

The chopper wheel as seen in Figure 22 was chosen as the flow disruptor. This design allows great flexibility in frequency selection. The wheel has four three-inch diameter holes configured for a duty cycle of 50%. That is the amount of time where thrust can pass is equal to when it is deflected. The wheel was driven using an electric

drill motor and transmission (Bosch model 1194AVSR). This allowed an RPM range of 0-1000 RPM. This RPM band corresponds to a pulsation frequency of 0 - 67 Hz. The drill motor speed was controlled using a household rheostat. The frequency was measured using an optical sensor (Monarch Instruments model ROS-5). The output of the optical counter was displayed on an oscilloscope (Tektronix model TDS 3034B) which allowed for the measurement of frequency as the output was a periodic digital signal.

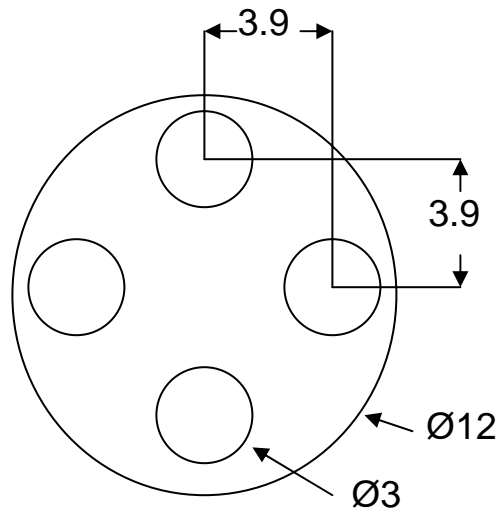


Figure 22. Chopper wheel, geometry and dimensions

Before each data run the chopper wheel was indexed so that an opening in the wheel was directly in front of the collector. The wheel was restrained with a thin metal wire to ensure it would stay stationary during the initial profile. The engine was then systematically cycled through throttle settings from idle to 100% and then returned to idle. Once at idle the chopper wheel was started spinning and a truncated throttle profile was followed from idle to 100% and then back to idle. This was accomplished at the

previously established optimal ejector downstream distance of six inches and then the ejector was removed to collect baseline thrust data. Figure 23 shows the chopper wheel as it was employed during this investigation.

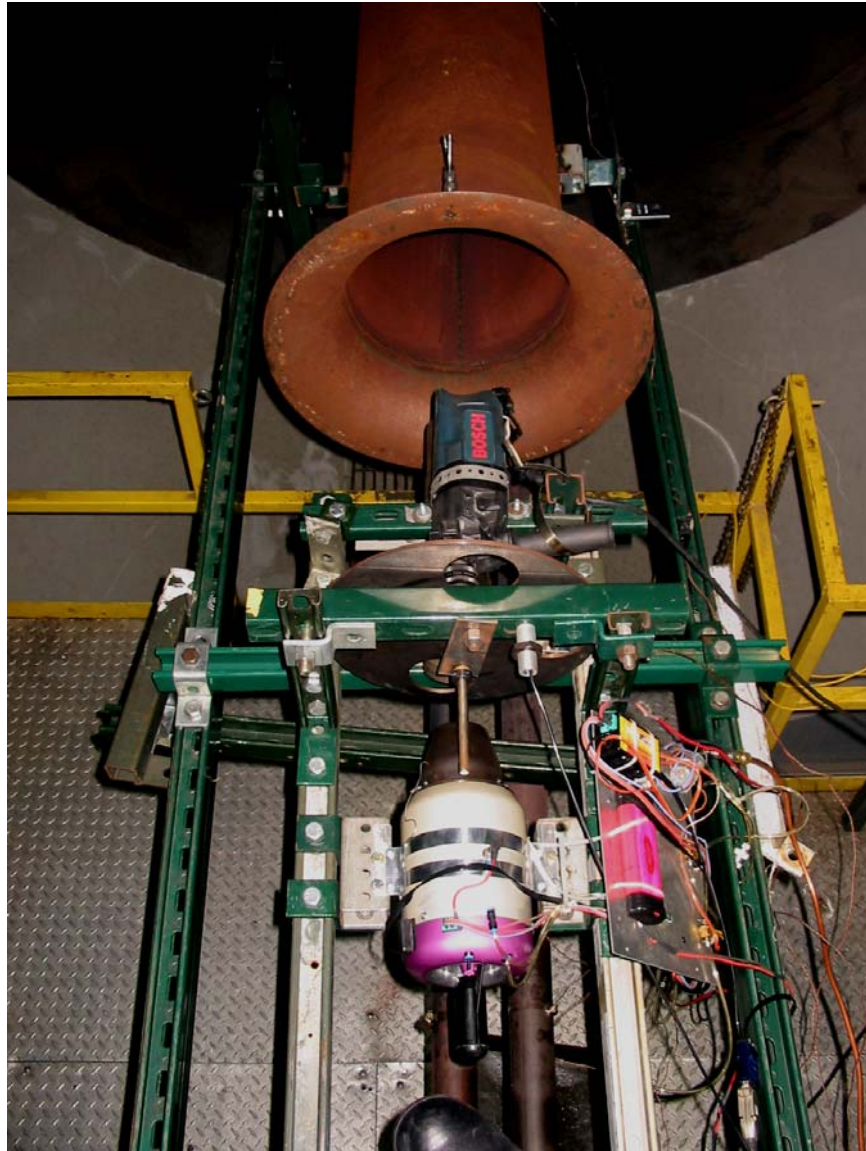


Figure 23. Series three X=6"

The basic unsteady ejector operation has been covered in an earlier section. The actual mechanics of the unsteady ejector's large augmentation deserves elaboration.

Recent advances in flow visualization techniques have given researchers the ability to better understand the mechanism by which the unsteady ejector creates such high thrust augmentation numbers.

With each wave being issued from the exit of a pulsejet or PDE there is a vortex established. This vortex, much like a smoke ring, forms just after the exit plane of the ejector. Figure 24 shows a steady jet on left and a pulsed jet on right. On the right hand picture one can clearly see the vortex ring established after the jet exit.

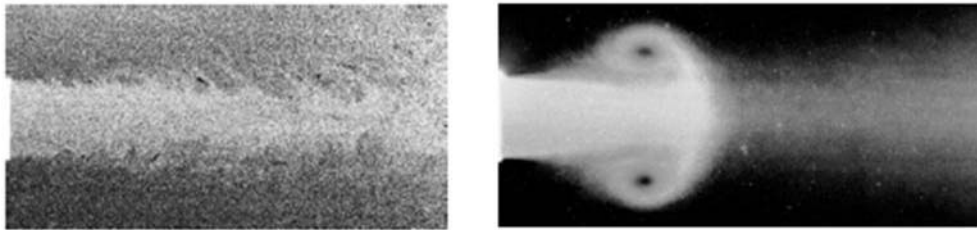


Figure 24. PIV flow visualization of a steady jet and a pulsed jet [2], by permission

From [3] “The vortex plays a critical role in determining thrust augmentation, through the physical mechanism is not understood... It is believed that the strong emitted shock, uniquely associated with the PDE pulse, has a large though currently not well understood, influence on the maximum attainable thrust augmentation.” Paxson’s [9] work which can be seen in Figure 25 shows the vortex ring with the profile of the ejector yielding peak augmentation overlaid.

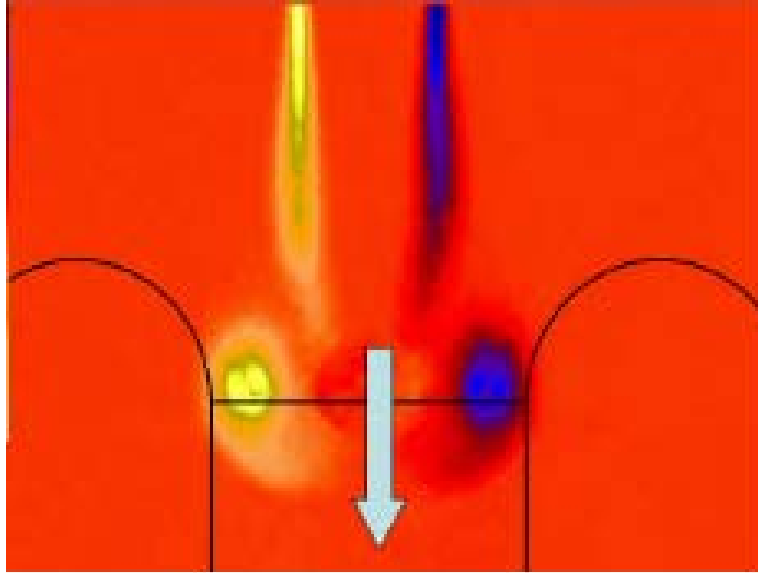


Figure 25. Vortex ring with ejector profile yielding peak augmentation [9]

Figure 26, shows the effect the chopper wheel had on the measured thrust. The chopper wheel was engaged at roughly 550 seconds while the engine was operating at 100% power. The engine RPM remains unchanged while thrust measured drops. Since the wheel has a 50% duty cycle the amount of thrust allowed to reach the ejector will be reduced. In addition to loss of thrust from duty cycle of the wheel is the inefficiency introduced by the chopper wheel and collector as a mechanism. It was observed that the chopper wheel and collector system caused a further reduction of 10% in thrust. Ideally the flow would have behaved as an unsteady source would and the augmentation created by this would have outweighed the losses from creating it.

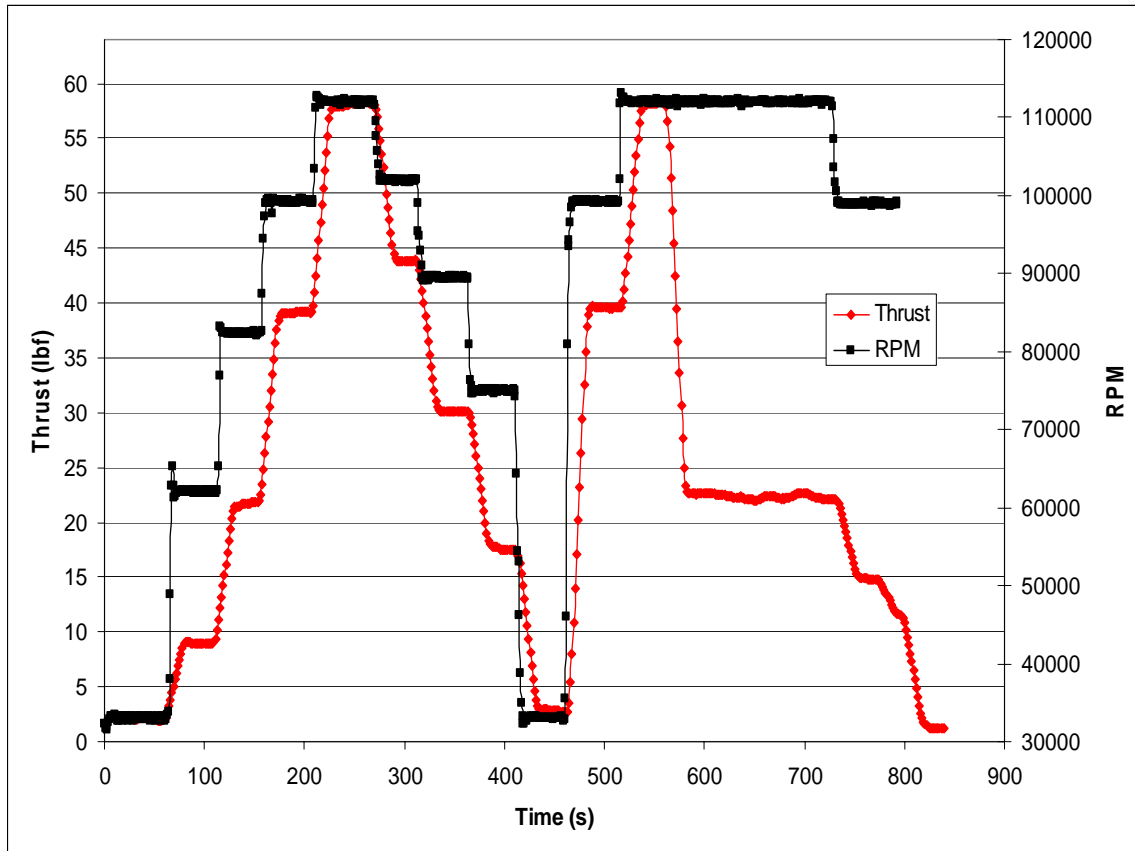


Figure 26. Series three thrust and RPM vs time, X=6''

How the mechanical losses for the chopper wheel collector assembly are affected by the ejector can be seen in Figure 27. The ejector amplifies the amount of thrust lost. Figure 28 clearly shows that there was no benefit to thrust by adding the collector and non-rotating wheel.

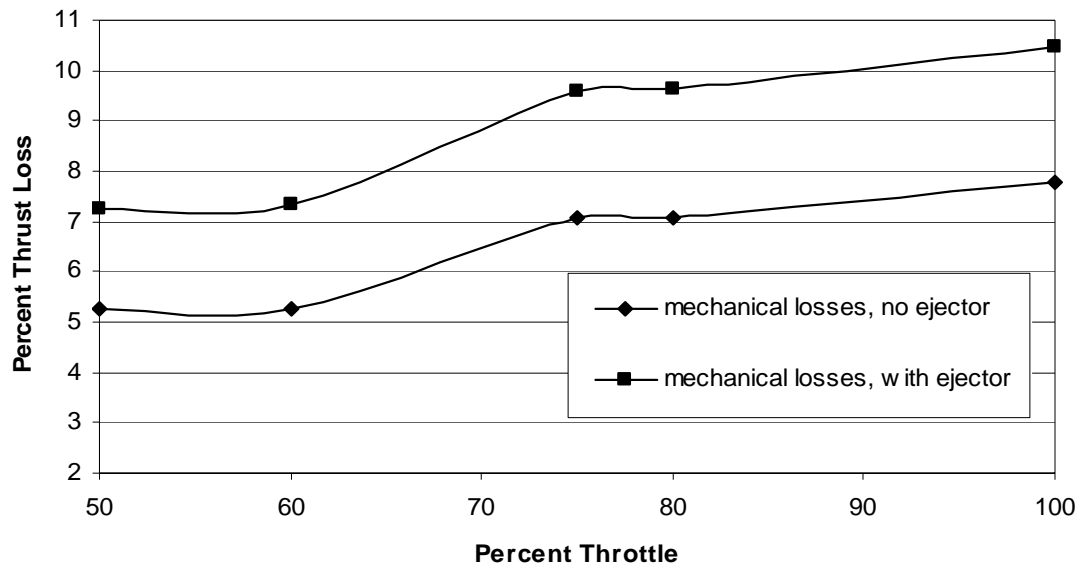


Figure 27. Mechanical losses vs. throttle percentage

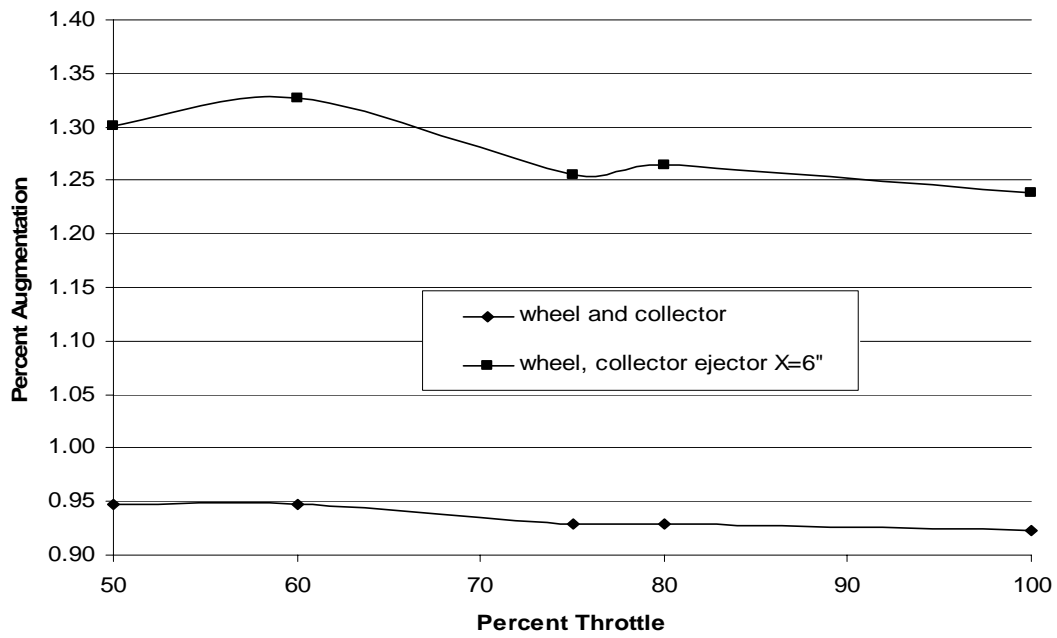


Figure 28. Variation of ϕ as a function of throttle for series three with the chopper not rotating

Less than expected thrust augmentation could be due to many things including incorrect research setup and wrong pulse frequency. Choutapalli, Krothapalli and Lourenco's [1] research was done at a significantly higher frequency. Increasing the frequency of the chopper wheel to mimic their band would increase the likelihood of finding a more optimal thrust augmenting system. Once the frequency band which produces good augmentation has been established then a more efficient system such as a bifurcating valve or resonance tube can be substituted for the chopper wheel-collector assembly. Resizing the ejector to create optimum thrust at this new frequency band would further enhance the performance.

Chapter Summary

Three series of data were collected, two focused on steady flow and the third attempted to create unsteady flow. Series one consisted of the engine and ejector. Series two was the same as one with the addition of the collector tube. Series three used the same engine, ejector and collector but now incorporated the chopper wheel. The methods and equations used to analyze the data including both the ideal and actual cases were discussed and shown. Results of the data series were presented in graphical form with comments on significant findings.

V. Conclusions and Recommendations

Conclusions

Both analytical and empirical evidence in this paper support the current thinking that an ejector driven directly by a gas turbine does not produce enough thrust augmentation when compared to unsteady system to overcome the increases in both weight and drag the system will impose on the aircraft. If peak performance for steady flow were desired further optimization could be done to this setup to improve augmentation. The ejector geometry could be configured to maximize thrust at peak engine MFR. Positioning the ejector at a distance of three engine nozzle exit diameters (D_p) downstream as shown with this work allows maximum thrust augmentation. However, Heiser's [6] analytic work shows the maximum ϕ that a steady ejector could produce is limited to two in the ideal case. While an ideal augments, to include unsteady ejector, can theoretically produce a much higher ϕ . Choutapalli, Krothapalli and Lourenco [1] have already demonstrated ϕ values in excess of 2.3 with $m_T/m_p=7$. Either by selection of an unsteady source as the ejector driver or by devising a way to make a steady source unsteady, clearly to achieve a value of thrust augmentation necessary to offset the penalties of the ejector system one must continue to explore the unsteady source.

Recommendations

This research and thesis lay an excellent groundwork for work on unsteady augmentation using this setup. With flight applicability in mind, it is not recommended

that further effort be invested in exploring peak steady augmentation with this turbine. There is a great deal of theoretical analysis that shows there is a large performance potential in unsteady sourced ejectors. Further effort should be given to developing a method to efficiently create unsteady engine flow. Choutapalli, Krothapalli and Lourenco [1] have had great success with a chopper wheel system. The pulse frequency at which their system shows peak augmentation is roughly four times higher than the frequency range explored in this research. The optimal steady diameter ratio, downstream distance and etc. will most assuredly not be the optimal for the unsteady efforts. Work should be continued in an effort to find a frequency and ejector geometry which produce maximum augmentation for this engine.

Collecting data from a flow visualization system focused on the stream exiting the collector will give a much better understanding what the flow entering the ejector looks like. Since it has been shown in multiple papers [1, 9, 12, 15] that the vortex ring size and strength are factors in the augmentation achieved, actual images of the flow should be high priority. Once the flow is characterized, an optimal frequency and ejector geometry can be determined.

After characterizing the stream from the collector with a flow visualization system, efforts can be focused on producing peak augmentation. Driving the chopper wheel at an increased speed will yield increased frequency. In addition, increasing the number of holes will not only increase the frequency but also synergistically increase the amount of thrust allowed to pass. Once a frequency band that shows good augmentation is arrived at a much simpler flow disruption system can be substituted. A resonance tube

or bifurcating valve each designed to operate at this optimal frequency could be used.

This coupled with an optimal geometry ejector will yield an attractive propulsion system for today and tomorrow's small airframes.

Bibliography

1. Choutapalli, Isaac M., Krothapalli, A., and Lourenco, L. M. "Pulsed Jet Ejector Characteristics," AIAA 2006-1019, *44th AIAA Aerospace Sciences Meeting and Exhibit*, Reno, NV, 09-12 Jan. 2006.
2. Choutapalli, Isaac M., Alkislar, M. B., Krothapalli, A., and Lourenco, L. M., "An Experimental Study of Pulsed Jet Ejector," AIAA 2005-1208, *43rd AIAA Aerospace Sciences Meeting and Exhibit*, Reno, NV, 10-13 Jan. 2005.
3. Paxson, Daniel, E., Litke, P., Schauer, F., Bradley, R., and Hoke, J. "Performance Assessment of a Large Scale Pulsejet-Driven Ejector System," AIAA 2006-1021, *44th AIAA Aerospace Sciences Meeting and Exhibit*, Reno, NV, 09-12 Jan. 2006.
4. Petty, James S. "Theoretical Performance Limits for Non-static Ejector thrust Augmentors," April 1980, AFAPL-TR-79-2120.
5. Amin, Sameh M. and Charles A. Garriss, Jr. "An Experimental Investigation of a Non-Steady Flow Thrust Augmenter." AIAA-1995-2802, *Proceedings of the 31st AIAA/ASME/SAE/ASEE Joint Propulsion Conference*, San Diego, CA, 1995.
6. Heiser, William H. "Thrust Augmentation," *Transactions of the ASME - Journal of Engineering for Power*, pages 75-82, Jan. 1967.
7. Lockwood, R.M. "Interim Summary Report on Investigation of the Process of Energy Transfer from an Intermittent Jet to Secondary Fluid in an Ejector-type Thrust Augmenter," Hiller aircraft report No. ARD-286, Mar. 1961.
8. Porter, J. L. and Squyers, R. A. "An Overview of Ejector Theory," AIAA-1981-1678, *Aircraft Systems and Technology Conference*, Dayton, OH, 11-13 Aug. 1981.
9. Paxson, Daniel, E., Wernet, M. P., and John, W. T., "An Experimental Investigation of Unsteady Thrust Augmentation Using a Speaker-Driven Jet," AIAA-2004-0092, NASA/TM-2004-212909, Feb. 2004.
10. Wilson, Jack. "The Effect of Pulse Length and Ejector Radius on Unsteady Ejector Performance," AIAA 2005-3829, *41st AIAA/ASME/SAE/ASEE Joint Propulsion Conference & Exhibit*, Tucson, AZ, 10-13 Jul. 2005.
11. Slack, John, D. *Branch Detonation of a Pulse Detonation Engine with Flash Vaporized JP-8*. MS Thesis. AFIT/GAE/ENY/07-D04. Department of Aeronautics and Astronautics, Air Force Institute of Technology, Wright Patterson AFB, OH. Dec. 2006.

12. Paxson, Daniel, E. Wilson, Jack, and Dougherty, Kevin, T., "Unsteady Ejector Performance: An Experimental Investigation Using a Pulsejet Driver," AIAA-2002-3915, *38th AIAA/ASME/SAE/ASEE Joint Propulsion Conference and Exhibit*, Indianapolis, Indiana, 07-10 Jul. 2002.
13. Paxson, Daniel, E. "Performance Enhancement of Unsteady Ejectors Investigated Using a Pulsejet Driver," 2002 Research and Technology, Glenn Research Center, NASA-TM-2003-211990.
14. Allgood, Daniel., Gutmark, E., Hoke, J., Bradley, R., Schauer, F., "Performance Measurements of Pulse Detonation Engine Ejectors," AIAA 2005-223, Jan. 2003.
15. Wilson, Jack., Sgondea, A., Paxson, D. and Rosenthal, B., "Parametric Investigation of Thrust Augmentation by Ejectors on a Pulsed Detonation Tube," AIAA 2005-4208, *41st AIAA/ASME/SAE/ASEE Joint Propulsion Conference & Exhibit*, Tucson, AZ, 10-13 Jul. 2005.
16. Oates, Gordon C., *Aerothermodynamics of Gas Turbine and Rocket Propulsion*. Third Edition, American Institute of Aeronautics and Astronautics, Inc., Reston, VA; 1997, pp. 192-195.
17. Mattingly, Jack D., *Elements of Gas Turbine Propulsion*. American Institute of Aeronautics and Astronautics, Inc., Reston, VA; 2005, pp. 363-368.
18. Mattingly, Jack D. and others, *Aircraft Engine Design*. Second Edition, American Institute of Aeronautics and Astronautics, Inc., Reston, VA; 2002, pp.95-121.

Vita

Captain David A. Hoffman was born, raised and educated in Virginia. He graduated Culpeper County High School in Culpeper, VA in June of 1996. As a cadet at Virginia Military Institute in Lexington, VA he earned a Bachelor of Science in Mechanical Engineering in May of 2000. He was commissioned through Detachment 880 Air Force ROTC the same month. In June 2000, he reported for duty at his first duty station, Electronic Systems Center Hanscom AFB in Massachusetts. At Hanscom he worked protected military satellite communications on the Milstar Command Post Replacement Program as a project engineer.

In July 2003, Lt Hoffman was reassigned to the 46th Test Group, 846th Test Squadron Holloman AFB New Mexico home of the World Land Speed Record. The Track operated a ten mile rocket sled test track and was responsible for weapons, hypersonic, crew safety and egress testing. Lt. Hoffman worked as a project manager for multiple weapons test projects. In January of 2005 Capt Hoffman was detailed to the 46th Test Group, 586th FLTS to manage classified weapons and flight test programs.

In September 2005, he entered the Air Force Institute of Technology Graduate School of Engineering and Management for his Masters of Science in Aeronautical Engineering. His emphases were in aircraft stability and control and also air weapons. Upon graduation in March 2007, he will attend USAF Test Pilot School as the class of 07B.

REPORT DOCUMENTATION PAGE				Form Approved OMB No. 074-0188	
<p>The public reporting burden for this collection of information is estimated to average 1 hour per response, including the time for reviewing instructions, searching existing data sources, gathering and maintaining the data needed, and completing and reviewing the collection of information. Send comments regarding this burden estimate or any other aspect of the collection of information, including suggestions for reducing this burden to Department of Defense, Washington Headquarters Services, Directorate for Information Operations and Reports (0704-0188), 1215 Jefferson Davis Highway, Suite 1204, Arlington, VA 22202-4302. Respondents should be aware that notwithstanding any other provision of law, no person shall be subject to a penalty for failing to comply with a collection of information if it does not display a currently valid OMB control number.</p> <p>PLEASE DO NOT RETURN YOUR FORM TO THE ABOVE ADDRESS.</p>					
1. REPORT DATE (DD-MM-YYYY) 03-13-2007		2. REPORT TYPE Master's Thesis		3. DATES COVERED (From – To) Sep 2005 - Mar 2007	
4. TITLE AND SUBTITLE Experimental Investigation of Turbojet Thrust Augmentation Using an Ejector				5a. CONTRACT NUMBER	
				5b. GRANT NUMBER	
				5c. PROGRAM ELEMENT NUMBER	
6. AUTHOR(S) Hoffman, David A., Capt, USAF				5d. PROJECT NUMBER	
				5e. TASK NUMBER	
				5f. WORK UNIT NUMBER	
7. PERFORMING ORGANIZATION NAMES(S) AND ADDRESS(S) Air Force Institute of Technology Graduate School of Engineering and Management (AFIT/EN) 2950 Hobson Way WPAFB OH 45433-7765				8. PERFORMING ORGANIZATION REPORT NUMBER AFIT/GAE/ENY/07-M13	
9. SPONSORING/MONITORING AGENCY NAME(S) AND ADDRESS(ES) AFRL/PRTC Attn: Dr. Fred Schauer 1790 Loop Road WPAFB OH 45433-7765				10. SPONSOR/MONITOR'S ACRONYM(S)	
				11. SPONSOR/MONITOR'S REPORT NUMBER(S)	
12. DISTRIBUTION/AVAILABILITY STATEMENT APPROVED FOR PUBLIC RELEASE; DISTRIBUTION UNLIMITED.					
13. SUPPLEMENTARY NOTES Advisor: Dr. Paul I. King, (937) 255-3636, ext 4628 paul.king@afit.edu					
14. ABSTRACT In recent years a significant number of commercially available micro turbines have become available. At the same time unmanned aerial vehicles and smart munitions have decreased in size while their endurance needs have increased. With these new platform requirements comes the need for a propulsion system with reliability, good endurance and low acoustic signature. There has been much research accomplished in the area of steady cold flow primary sources, but little experimental work has been done using a gas turbine as a steady flow hot source. This investigation concerns the performance of an ejector driven by a small gas turbine. Aircraft applicability was a deciding factor in test geometry. Varying both engine throttle and the ejector's downstream distance resulted in peak augmentation values of nearly 1.4.					
15. SUBJECT TERMS Ejectors(fluid); turbojet engines; thrust augmentation; exhaust gas ejectors					
16. SECURITY CLASSIFICATION OF:		17. LIMITATION OF ABSTRACT UU	18. NUMBER OF PAGES 71	19a. NAME OF RESPONSIBLE PERSON Dr. Paul I. King (ENY)	
ABSTRACT U	c. THIS PAGE U			19b. TELEPHONE NUMBER (Include area code) (937) 255-6565, ext 4628; e-mail: paul.king@afit.edu	

Standard Form 298 (Rev. 8-98)
Prescribed by ANSI Std. Z39-18